The role of GlpR repressor in *Pseudomonas putida* KT2440 growth and PHA production from glycerol.

Escapa, I. F., del Cerro, C., García, J.L., and Prieto, M.A. *

Environmental Biology Department, Centro de Investigaciones Biológicas, CSIC, Ramiro de Maeztu 9, 28040 Madrid, Spain.

Running title: *Pseudomonas putida* growth and PHA production from glycerol

Key words: *Pseudomonas putida* KT2440, polyhydroxyalkanoates, glycerol

*Corresponding author. Mailing address: Environmental Biology Department, Centro de Investigaciones Biológicas, CSIC, Ramiro de Maeztu 9, 28040 Madrid, Spain. E-mail: auxi@cib.csic.es.

Summary

Pseudomonas putida KT2440 has evolved a tightly regulated system for metabolizing glycerol implying a prolonged growth lag-phase. We have learnt that this long lag-phase can be avoided by the addition of small amounts of some growth precursors. The addition of 1 mM octanoic acid as co-feeder completely eliminated the lag-phase, resulting in an improvement, in terms of invested time, of both growth and polyhydroxyalkanoates (PHA) accumulation. To investigate this phenomenon, we have followed co-metabolic approaches combined with mutations of the specific and global regulatory networks connecting the glycerol catabolism and PHA synthesis. We have established that the GlpR regulator represses glycerol catabolism in this strain, being responsible for the long lag-phase. Based on this finding we have created a *glpR* knock-out mutant of *P. putida* KT2440 showing a reduction of the lag phase of 10 hours when cultured on glycerol. The production of PHA in this strain was enhanced resulting in a higher final yield in terms of PHA accumulation. In a high C/N unbalance nutrient situation, such as C/N ratio of 80 mol/mol, *P. putida* KT40GlpR was able to produce PHA as 39 ± 5% of CDW after 46 hours of growth, while the wild type strain accumulated 25 ± 6% of CDW. This improved glycerol consuming strain will be also very useful for the efficient transformation of glycerol into other valuable products.

Introduction

Polyhydroxyalkanoates (PHAs) are storage bacterial polyesters accumulated in the cytoplasm as carbon and energy reserve materials that are synthesized when there is an unbalanced situation between the carbon supply and another essential nutrient, such as nitrogen or phosphorus (Madison and Huisman, 1999; Prieto, *et al.*, 2007; Rehm,

2010). These thermoplastic polymers have been proposed as a green alternative to the petroleum derivate material industry because of their biodegradable and recyclable nature (Luengo, *et al*., 2003; Chen, 2009; Gao *et al*., 2011). Large-scale production of PHAs implies elevated costs due to, not only to the fermentation and separation process (Sun *et al*., 2007; Elbahloul and Steinbüchel, 2009; Martínez *et al*., 2011), but also to the availability of appropriated carbon sources. Therefore, research efforts have been focused in the use of low cost industrial residues as fermentative substrates for PHA production (Solaiman *et al*., 2006; Serafim *et al*., 2008; Castilho *et al*., 2009). Glycerol is a by-product of biodiesel industry that has been postulated as one of the most attractive raw materials for the bacterial production of value-added products; it has been analyzed as substrate for PHA synthesis in natural PHA producers (Bormann and Roth, 1999; Cavalheiro *et al*., 2009; Reddy *et al*., 2009; Ibrahim and Steinbüchel, 2010; Kawata and Aiba, 2010), including Pseudomonads (Huijberts *et al*., 1992; Ashby *et al*., 2005; Solaiman *et al*., 2006), as well as in recombinant *Escherichia coli* carrying *pha* biosynthetic genes (Mahishi *et al*., 2003; Nikel *et al*., 2008). Some of the more extensively studied natural PHA producers are the *Pseudomonas* strains, especially *Pseudomonas putida* KT2440, a mcl-PHA producer that is a prototype microorganism for biotechnological purposes with a vast potential for environmental and industrial applications (Nelson *et al*., 2002; Escapa *et al*., 2011).

The improvement of glycerol utilization in bacterial PHA producers implies the study of the metabolic steps involve in glycerol catabolism, as well as their links with the central metabolic routes that connect glycerol dissimilation with PHA synthesis (Fig. 1). Within the *Pseudomonas* species glycerol uptake and metabolism have been biochemically characterized in the opportunistic human pathogen *P. aeruginosa*, in which glycerol can be utilized as an important carbon source within the lung (Williams

et al., 1994). In this strain the first step in glycerol uptake is mediated by OprB; an outer-membrane porin which is over-expressed under glycerol limitation (Williams *et al*., 1994). A glycerol facilitator (GlpF), also involved in glycerol transport, is closely associated with a glycerol kinase (GlpK) that converts glycerol to glycerol 3-phosphate (G3P) (Fig. 1) (Schweizer *et al.*, 1997). Then, G3P is transformed to dihydroxyacetone phosphate (DHAP) by a cytoplasmic-membrane-associated G3P dehydrogenase (GlpD) (Schweizer and Po, 1994), and the DHAP is further catabolized by a branch of the Entner-Doudoroff (ED) pathway (McCowen *et al*., 1981; Cuskey and Phibbs, 1985). The *glp* operons (*glpFK* and *glpD*) of *P. aeruginosa* are negatively regulated by GlpR (Schweizer and Po, 1996). Nevertheless, our current knowledge concerning glycerol catabolism in *P. putida* is still very limited and it has been mainly based in its genome annotation (KEGG Pathway Database: http://www.genome.jp/kegg/pathway.html; Nelson *et al*., 2002) and in the information derived from *P. aeruginosa* (Schweizer and Po, 1996). Figure 1 summarizes the proposed interconnections between glycerol catabolism and the other biochemical pathways (*e.g.*, carbohydrate catabolism, ED pathway, fatty acid oxidation and *de novo* synthesis, and PHA cycle) in *P. putida*, as well as the regulatory network driving these routes.

In this work, we have combined different co-metabolic strategies with the manipulation of the specific and global regulatory networks to improve growth and PHA production in *P. putida* KT2440 when glycerol is used as the main carbon source. Our results demonstrate the key role played by the GlpR regulator in the optimization of PHA production from glycerol.

Results

Analyses of the P. putida *KT2440 growth profiles as function of the carbon source: The lag-phase of glycerol culture.*

Fatty acids are currently used as preferred substrates for the microbial mcl-PHA synthesis in Pseudomonads (Solaiman *et al*., 2006; Sun *et al*., 2007; de Eugenio *et al*., 2010b). To optimize the PHA production on non preferred industrial raw precursors, the growth of *P. putida* KT2440 on fatty acids and other carbon sources has been compared. Thus, quantitative growth assays were performed in M63 minimal medium in microwell plates using diverse carbon and energy sources that are incorporated to the central metabolism at different stages (Fig. 2). It is worth to mention that PHA production in *P. putida* KT2440 on octanoate can be achieved even under no nutrient limitations (Wang and Nomura, 2010; Follonier *et al*., 2011). However, PHA accumulation in KT2440 requires a carbon/nitrogen (C/N) unbalance when PHA non related precursors such as gluconate are used as carbon sources (Follonier *et al*., 2011). This phenomenon is shown by the remarkable difference in the OD_{630} reached by cells growing in octanoate (from 9 hours on) comparing to the rest of the growth curves. The apparent growth rate in octanoate during the first 9 hours (*i.e.*, when PHA accumulation does not influence OD_{630}) is 0.132 h^{-1}. As expected, this is the highest growth rate achieved from all the assayed carbon sources. Acetate and pyruvate showed the lowest growth rates, *i.e.*, μ=0.024 h^{-1} and μ=0.041 h^{-1}, respectively. When fructose or glycerol were used as the sole carbon source the growth rates were μ=0.053 h^{-1} and μ=0.058 h^{-1}, respectively, but cultures in glycerol showed a long lag-phase (up to 15 hours). The second highest rate corresponded to citrate (μ=0.090 h^{-1}).

Thereafter, flask experiments were also performed to confirm these data (Table 1). When octanoate was used as substrate *P. putida* KT2440 produced around a 20% of PHA (% CDW), in agreement with the production observed when fatty acids are used as

carbon sources in a C/N balanced medium (Follonier *et al*., 2011). Final biomass free of PHA on octanoate was 0.76 g/l (g/l measured as total cell dry weight (CDW) minus g/l of PHA). As expected, PHA was not detected when any of the carbon sources different to fatty acid were assayed. Acetate and pyruvate reached the lower biomass values (0.54 g/l and 0.63 g/l, respectively), while the highest yields corresponded to fructose and glycerol (0.94 g/l and 0.93 g/l, respectively). Despite glycerol does not provide an elevated growth rate, the high biomass yield reached with this substrate makes it a suitable carbon source for fermentative processes (Pachauri and He 2006; Solaiman *et al*., 2006). However, for scaling up purposes, shorting the extremely long lag-phase observed in glycerol is demanded.

Fatty acid based co-feeding strategies for stimulation of glycerol growth versus *PHA and TCA (tricarboxylic acid) cycles activities.*

To design fermentation strategies for an efficient mcl-PHA production on glycerol in *P. putida* KT2440 we took into account that PHA metabolism and β-oxidation pathway are coordinately regulated in *P. putida* KT2440 via PhaD transcriptional activator (de Eugenio *et al*., 2010b). PhaD allows the efficient transcription of *pha* genes when fatty acids or related intermediates of the β-oxidation pathway are available (de Eugenio *et al*., 2010b). Moreover, we took advantage of the fact that co-metabolism with fatty acids has been applied to increase PHA production yields (Lenz *et al*., 1992; Zinn *et al*., 2001; Escapa *et al*., 2011).

Based on these observations, we have analyzed the effect of fatty acid co-feeding on growth and PHA production when cells of *P. putida* KT2440 were cultured in glycerol as carbon and energy source under PHA production conditions (*i.e.*,

145 unbalanced high C/N ratio, hereafter used in this study as culture conditions to analyze
146 PHA accumulation) (Fig. 3A). In the cultures induced with octanoate we have observed
147 a higher final OD_{630nm} that would be traduced in an enhanced growth, but also could be
148 owing to the accumulation of a higher amount of PHA. Even more interesting was the
149 unexpected observation that the lag-phase on glycerol was exceptionally reduced due to
150 the presence of octanoate. When PHA accumulation was analyzed after 46 h of culture
151 we observed a production of 19 ± 2% of CDW in 40 mM glycerol *vs*. 27 ± 2% in 40
152 mM glycerol plus 1 mM octanoate. This effect was also detected in the presence of 0.1
153 mM octanoate.

154 These data allowed us to speculate about a putative role of the PHA cycle for
155 controlling the metabolism of glycerol via initial transformation of octanoate into PHA.
156 To study this possibility, we analyzed the growth profile of *P. putida* KT40C1ZC2, a *P.*
157 *putida* KT2440 mutant unable to accumulate the polyester due to a deletion in the
158 *phaC1ZC2* genes, coding for the PHA synthases and depolymerase (Fig. 3B, see
159 Experimental procedures for details of the strain construction). We observed in the PHA
160 minus mutant a similar octanoate effect over glycerol lag-phase, demonstrating that this
161 phenomenon is not linked to the activity of PHA cycle.

162 By serendipity, we had observed that *P. putida* KTH2, one of our collection
163 strains, was not able to growth using octanoate as substrate (Fig. 4). When we tested the
164 effect of octanoate on this strain, we observed that it was not able to stimulate glycerol
165 growth (Fig. 4) suggesting that this stimulation was linked to the catabolism of
166 octanoate. *P. putida* KTH2 is a *P. putida* KT2442 derivative bearing an *hpaBC* cassette
167 encoding the *E. coli* 4-HPA hydroxylase introduced into the chromosome via mini-
168 transposon (Prieto *et al*., 1996). Remarkably, other transconjugants of our collection
169 bearing the same mini-transposon were able to growth in octanoate (data not shown)

suggesting that the mini-transposon integrated in KTH2 had produced a disruption of a key gene for fatty acid catabolism. In fact, we have now demonstrated that the mini-transposon integration has generated an *aceA* disruption mutant in *P. putida* KTH2 (see Experimental procedures section). The *aceA* gene encodes the isocitrate lyase and its deletion impairs fatty acid metabolism due to a blockage of the glyoxylate bypass of the TCA cycle (Kornberg and Krebs, 1957; Kornberg, 1966). Figure 4A shows that octanoate induction over glycerol consumption is nearly undetectable in *aceA*$^-$ mutant strain compared to the wild type. This result suggests that either octanoate degradation to central intermediates from TCA cycle or gluconeogenesis is required to activate glycerol utilization in *P. putida*. This effect was confirmed by complementation of the *aceA*$^-$ mutant, showing that *P. putida* KTH2 phenotype was exclusively due to the *aceA* mutation (Fig. 4B). Interestingly, despite of the lack of octanoate induction over glycerol growth in the strain KTH2, the analysis of PHA production from glycerol showed that both strains (KT2442 and KTH2) accumulated PHA more efficiently when glycerol is supplemented with octanoate (Fig. 4C). This result suggests that although octanoate cannot support the growth of KTH2, it can contribute to the synthesis of PHA through the PHA cycle.

Glycerol catabolism in P. putida *KT2440 relies on an active ED pathway.*

The results described above suggested that the effect of octanoate on glycerol metabolism could rely either on a global activation of the cell energy state or on the generation of specific metabolites or cofactors needed for the activation of glycerol metabolism. To study this effect we compared growth and PHA accumulation of *P. putida* KT2440 under low nitrogen conditions (M63 0.1N media) using glycerol as the main carbon source with a small dosage of glucose or octanoate as co-feeders (Fig. 5).

These results were also compared with that obtained from *P. putida* KT2440 cells growing exclusively with octanoate or glucose as carbon sources (Fig. 5). We observed similar growth stimulation pattern, this is, significant reduction of the initial lag-phase in glycerol, when carbon equimolar concentrations of octanoate or glucose were added to the glycerol growth media. As expected, in both cases cultures reached a higher final total biomass (around 1 g/l) than that observed when glycerol is used as the sole carbon source (0.8 ± 0.04 g/l) (Fig. 5C). Concerning PHA accumulation levels, when 1 mM octanoate was added to the media the cells accumulated a higher amount of PHA (31 ± 1% of CDW) than the cells using only glycerol as carbon source (21 ± 4% of CDW), or when glycerol was co-feeded with glucose (20 ± 2% of CDW). This PHA increase observed in the presence of octanoate could be due to an increment of available PHA synthase substrates in the cytoplasm directly generated by β-oxidation of octanoate. This result is in agreement with the higher amount of 3-hydroxyoctanoate (C8) monomers present in this polyester compared to that produced from other carbon sources (see Supporting information Fig. S1). Summing up, co-feeding of glycerol containing media with a non-related PHA carbon source like glucose stimulate glycerol growth, but not PHA accumulation in *P. putida* KT2440, whereas co-feeding with a related PHA carbon source like octanoate stimulate both glycerol growth and PHA production.

As detailed in Figure 1, once glycerol is transported into the cells, activated to G3P and transformed into DHAP by the action of the enzymes encoded by *glp* genes, it should be further catabolised by a branch of the ED pathway (McCowen *et al.*, 1981; Cuskey and Phibbs, 1985). This path connects the catabolic routes for glucose and glycerol assimilation to the gluconeogenesis and fatty acid catabolism via pyruvate (Fig. 1). Therefore, the stimulating phenotype observed for the cells growing in glycerol co-

feed with a low amount of glucose or octanoate must correlate with the activation of the ED route. To demonstrate this assumption, glyceraldehyde-3-phosphate dehydrogenase (GAPDH) enzymatic activity has been assayed after 6 and 22 hours of growth of *P. putida* KT2440 in different conditions (Table 2). Interestingly, when octanoate was used as carbon source, only a basal level of GAPDH activity was detected. As expected, a basal activity was detected after 6 hours in glycerol due to the lag-phase. After 22 hours of culturing in glycerol, the GAPDH enzymatic activity is more than tenfold compared to the basal level and in the range of the observed for glucose (Table 2). The induction of GAPDH activity is also evident when *P. putida* KT2440 strain was grown in glycerol in the presence of glucose or octanoate as inducers. Taking into account that octanoate is not metabolized through the ED pathway, and therefore, it does not induce GAPDH, this result suggests that the co-feeding effect cannot be ascribed specifically to a pre-activation of the ED pathway by fatty acids. Nevertheless, it is important to notice that the observed concomitant activation of the catabolic NAD^+ dependent GAPDH with glycerol utilization demonstrates that an efficient glycerol catabolism in *P. putida* KT2440 relies on an active ED pathway. Therefore, we can conclude that the ED pathway is activated due to glycerol metabolism and not to fatty acid metabolism.

Inactivation of the transcriptional regulator GlpR allows P. putida *KT2440 to use glycerol as optimal PHA and growth precursor.*

According to Figure 1 we had proposed that GlpR and HexR transcriptional regulators, as well as Crc global carbon metabolism post-transcriptional regulator, form part of the regulatory network controlling the central metabolic pathways connected to ED route, including glycerol route. To investigate their role in the co-feeding activation effect, the *glpR*, *hexR* and *crc* genes were deleted in *P. putida* generating single and

245 double mutant strains (see Experimental procedures for details in the constructions).
246 When the effect of these deletions over *P. putida* KT2440 glycerol growth were
247 analyzed (Fig. 6), we observed that the *glpR*$^{-}$ mutant (strain KT40GlpR) did not show
248 the long lag-phase in glycerol detected in the wild type strain. However, the deletion of
249 *hexR* gene (strain KT40HexR) did not change the growth curve of *P. putida* KT2440 on
250 glycerol and moreover, the *hexR*$^{-}$-*glpR*$^{-}$ double mutant (strain KT40HexR-GlpR)
251 behaved as the single *glpR*$^{-}$ mutant (strain KT40GlpR) suggesting that HexR is not
252 involved in the glycerol lag-phase effect. Finally, the mutation on *crc* (strain KTCRC)
253 did not modify the long lag-phase on glycerol, suggesting that, CRC is not involved in
254 this phenomenon.

255 The stimulatory effect on glycerol growth observed in the absence of GlpR was
256 confirmed by measuring the activity of the GAPDH in the KT40GlpR mutant (Table 2).
257 As expected, GAPDH activity is activated at 6 hours of growth when cells of *P. putida*
258 KT40GlpR were cultured in glycerol (Table 2). It is interesting to notice that the
259 GAPDH expression is not constitutive in the KT40GlpR mutant since it remains at basal
260 levels when cells are cultured in octanoate as the only carbon source. This result
261 demonstrates that although the activation of ED pathway depends of the presence of
262 glycerol it is not directly regulated by GlpR.

263 It has been proposed that in *P. putida* KT2440, *glpR* controls the expression of
264 the *glp* genes (Fig. 1). According to genome annotation, the g*lpF* gene coding for the
265 glycerol facilitator and the *glpK* gene coding for the glycerol kinase seem to form an
266 operon located upstream of *glpR*, whereas the *glpD* gene encoding the glycerol-3-
267 phosphate dehydrogenase is located downstream of *glpR* (Fig. 7A). To confirm the
268 implication of GlpR in the expression of these genes during the lag-phase (*i.e.*, during
269 the first 3 hours of growth) we have determined by qRT-PCR the expression of *glpF* in

the wild type *P. putida* KT2440 strain and in the *glpR*$^{-}$ mutant under different culture conditions. No statistically significant differences in *glpF* transcription levels during the lag-phase were detected when *P. putida* KT2440 cells growing in 15 mM octanoate as the sole carbon source were compared with 40 mM glycerol as unique substrate, suggesting that the lag-phase is due to a poor induction of the *glpFK* operon (Fig. 7B). However, when *P. putida* KT2440 was grown in a mixture of 40 mM glycerol plus 1 mM octanoate, the *glpF* expression increased, showing that the presence of octanoate could contribute to the induction of the *glpFK* operon and thus, to activate glycerol consumption (Fig. 7B). The finding that the expression of *glpF* was constitutive (non-repressed) in the KT40GlpR mutant strain in all the conditions assayed (Fig. 7B) suggests that GlpR is a repressor and agrees with the absence of lag-phase in this mutant when growing in glycerol. The low expression of *glpF* gene in the wild type strain growing on octanoate implies that the system needs the presence of glycerol in the medium, because the ligand of GlpR repressor is a metabolite derived from glycerol, very likely the G3P. We have also observed that *glpK* expression is constitutive (non-repressed) in the GlpR mutant when growing in glycerol or octanoate separately (Fig. 7C). However, in the wild type strain *glpK* expression is repressed in the presence of octanoate and partially de-repressed in the presence of glycerol. The mixture of both substrates fully activates *glpK* expression in both strains, supporting the idea that the system is also activated by co-feeding with octanoate.

In addition, we have analyzed how the deletion of GlpR repressor affects bacterial growth and PHA accumulation using glycerol as carbon source and small dosages of octanoate or glucose as co-feeding inducers (Fig. 8). As predicted, the initial growth long lag-phase disappears in KT40GlpR independently of inducer addition (Fig. 8A and 8B). While *P. putida* KT2440 wild type strain achieved a biomass of only 0.50

± 0.06 g/l after 22 hours of culture using glycerol as the sole carbon source (Fig. 5C), the KT40GlpR mutant strain reached 0.90 ± 0.01 g/l (Fig. 8C). Furthermore, *P. putida* KT40GlpR mutant strain growing in glycerol accumulates a higher amount of PHA (34 ± 6% of CDW) (Fig. 8C), than the wild type strain (21 ± 4% of CDW) (Fig. 5C). This suggests that *glpR* inactivation in *P. putida* KT2440 not only results in a more rapid use of glycerol, but also allows a higher accumulation of PHA polymer, very likely due to an increase in the availability of central metabolites that are channeled to the polyester synthesis.

Finally, for optimizing the PHA production, we have analyzed the PHA accumulation in KT40GlpR mutant strain at high C/N ratio. Wild type and mutant cells were cultured in 0.1N M63 medium containing 40 mM glycerol (C/N ratio of 40 mol/mol) or 80 mM glycerol (C/N ratio of 80 mol/mol) (Table 3). In this deeply C/N unbalance nutrient situation *P. putida* is able to reach high levels of PHA without compromise cell growth. The strain *P. putida* KT40GlpR accumulates higher levels of PHA than the wild type strain not only at 22 h of growth, when the wild type strain does not produce PHA, but even after 46 h reaching 39 ± 5% of CDW, nearly double of the value achieved by the wild type strain.

Discussion

In the last decades we have attended to an important development of biodiesel industry and, therefore, to a decrease in the cost of some by-products generated in its synthesis (Solaiman *et al*., 2006; da Silva *et al*., 2009). The crude glycerol obtained as the main derived sub-product of the industrial production of biodiesel cannot be used for direct food and cosmetic uses due to its low-grade purification quality (Johnson and

319 Taconi, 2009). Thus, the development of new uses for this waste material will
320 sensitively reduce the biodiesel production costs. As a result, glycerol has become a
321 very attractive raw material in bacterial fermentation processes. The use of glycerol for
322 microbial PHA synthesis has been analyzed in wild type microorganisms (revised in
323 Gomez *et al*., 2012), such as *Zobellella denitrificans*, *Methylobacterium rhodesianum*,
324 *Ralstonia eutropha*, several *Pseudomonas* strains, and *Bacillus* sp. (Bormann and Roth,
325 1999; Solaiman *et al*., 2006; Ibrahim and Steinbüchel, 2009; Reddy *et al*., 2009;
326 Ibrahim and Steinbüchel, 2010). Glycerol has also been used as substrate for PHB
327 synthesis in recombinant *E. coli* carrying the PHB biosynthetic genes (Mahishi *et al*.,
328 2003; Nikel *et al*., 2008). PHAs obtained from glycerol were reported to show
329 differences in terms of molecular weight with polymers synthesized from other
330 substrates, and these differences are species dependent (Ashby *et al*., 2005; Cavalheiro
331 *et al*., 2009; Reddy *et al*., 2009; de Almeida *et al*., 2010).

332 In this work we have constructed a *P. putida* KT2440 derivative strain in which
333 the deletion of *glpR*, the transcriptional repressor driven *glp* genes regulation, provides
334 an efficient PHA accumulation using glycerol as growth and polyester precursor. We
335 have demonstrated that GlpR regulator represses glycerol catabolism in this strain, and
336 that this repression appears to be responsible of the long lag-phase observed when cells
337 were cultured in glycerol as the sole carbon and energy source (Fig. 2).

338 Glycerol metabolism has not been studied in detail in the environmental model
339 strain *P. putida* KT2440 and therefore, only few biochemical and genetic data were
340 available on this issue. According to genome annotation, the *glp* cluster (PP_1076 to
341 PP_1073) exhibits a high degree of sequence identity of about 83%, 82%, 80% and 72%
342 for *glpF*, *glpK*, *glpR* and *glpD* genes, respectively, with the homologous genes of *P.*
343 *aeruginosa* (PA_3581 to PA_3584) (KEGG Pathway Database:

344 http://www.genome.jp/kegg/pathway.html). Although some preliminary studies
345 postulated the presence of a positive regulator (GlpR) controlling *glp* gene expression in
346 *P. aeruginosa* (Cuskey and Phibbs, 1985), this observation was subsequently denied
347 because it was demonstrated the existence of two *glp* operons (*glpFK* and *glpD*)
348 negatively regulated by GlpR (Schweizer and Po, 1996), in agreement with the
349 regulation of the *glp* operon in *E. coli* that is repressed by GlpR (Zeng and Larson,
350 1996). The *glp* operon of *E. coli* is repressed by GlpR in absence of intracellular
351 glycerol (specific repression), although this regulation is thought to be leaky, since
352 GlpK is required to produce G3P that is the true effector of the system (Applebee *et al.*,
353 2011). G3P has been also proposed as inducer of *P. aeruginosa glp* regulon (Schweizer
354 and Po, 1996). Schweizer and Po (1996) have identified some putative GlpR binding
355 sites upstream *glpF* and *glpD* genes of *P. aeruginosa* based on their identity with the *E.*
356 *coli glp* operator consensus sequences. We have identified a similar operator site
357 upstream the *glpF* gene of *P. putida* KT2440 (data not shown). The Mg^{2+}-ATP-
358 dependent phosphorylation of glycerol to G3P catalyzed by the glycerol kinase (GlpK)
359 is the key regulatory and rate-limiting step in glycerol utilization in *E. coli* (Zwaig *et al.*,
360 1970). GlpK activity is affected by multiple factors, *i.e,* ATP concentration (Applebee *et*
361 *al*., 2011), allosteric inhibition by fructose-1,6-bisphosphate (FBP) (Zwaig and Lin,
362 1966; de Riel and Paulus, 1978), and inhibition by the IIAGlc cytosolic component of
363 the bacterial phosphotransferase system (Novotny *et al.*, 1985). These factors generated
364 by the metabolism or the uptake of glucose inhibit GlpK activity during growth on
365 glucose and other catabolically preferred substrates.

366 The implications of GlpK and G3P in the regulation of the first step in the
367 metabolism of glycerol in *P. putida* have not been demonstrated yet but the results
368 shown in figure 7 suggest that the GlpR driven control of *glp* genes requires the

369 presence of glycerol in the culture medium, very likely because a derived metabolite of
370 glycerol is the GlpR effector. Our results are also in agreement with the studies of Wang
371 and Nomura (2010) showing that the expression of *glpF*, *glpK* and *glpD* genes in *P.*
372 *putida* KT2440 was higher in cells cultured in glycerol than in other carbon sources.
373 Finally, it has been demonstrated that mutations in the genes involved in the
374 phosphotransferase system of this strain altered the growth on glycerol, suggesting that
375 the glycerol catabolism of *P. putida* is controlled by a complex regulatory network
376 (Velazquez *et al*., 2007).

377 It was early suggested that glycerol catabolism relies on a functional and active
378 ED pathway in *P. aeruginosa* (Blevins *et al*., 1975; Heath and Gaudy, 1978) and in *P.*
379 *putida* (Aparicio *et al*., 1971; Vicente and Cánovas, 1973). Heath and Gaudy (1978)
380 proposed that glycerol metabolism depends on the activation of GAPDH and, therefore,
381 on an active metabolism of the hexosephosphate derivatives. This hypothesis is in
382 agreement with the increase of GADPH activity observed when glycerol is efficiently
383 used by the *P. putida* wild type strain in the presence of co-feeding inducers or by the
384 KT40GlpR mutant strain in the absence of inducers (Table 2).

385 The expression of the main metabolic steps of the phosphorylative branch of
386 carbohydrates metabolism and ED pathway in *P. putida* KT2440 is tidy regulated (del
387 Castillo *et al*., 2008) (summarised in Fig. 1). HexR is a transcriptional repressor
388 controlling some key steps of these routes, including the catabolic GAPDH enzyme
389 codified by *gap-1* gene (Daddaoua *et al*., 2009). The specific inducer of HexR is 2-keto-
390 3-deoxy-6-P-gluconate (KDPG), an intermediate in the ED pathway that could play a
391 relevant role as signalling molecule in catabolite repression (Daddaoua *et al*., 2009;
392 Rojo, 2010). Whether the connection between the metabolism of carbohydrates and
393 glycerol can be also ascribed in *P. putida* to FBP as occurs in *E. coli* via GlpK

394 regulation (see above) should be further analyzed.

395 The importance of Crc mediated catabolic repression in the ED pathway has also
396 been reported, since several genes of this route, including *gap-1*, are over-expressed in a
397 *P. putida* KT2440 *crc* mutant (Moreno *et al*., 2009). Furthermore, Browne *et al*. (2010)
398 have identified in this strain several Crc recognition motifs upstream *glpF*, *oprB-1* and
399 *gap-1* genes. Although this finding suggested that Crc might be also involved in
400 controlling the lag-phase observed in glycerol cultures, we did not observe a shortened
401 lag-phase in a *P. putida crc*$^{-}$ mutant under the growth conditions assayed in this work.

402 Our results have demonstrated that GlpR is a key regulator controlling glycerol
403 catabolism, but we cannot exclude the implication of other regulators (*e. g.*, HexR and
404 Crc), some enzymes (*e. g.*, GlpK and GADPH) and some metabolites (*e. g.*, G3P, ATP
405 and FBP) in this complex regulatory network. In fact, we propose that the effect of
406 octanoate and glucose might be due to an activation of the basal GlpK activity causing
407 an increase in the levels of G3P inducer. This activation is not only driven at the
408 transcripcional level (Fig. 7C), but also might be due to a punctual increase of the ATP
409 levels that could active GlpK, which would produce a small amount of G3P for opening
410 the circuit. In agreement with this sugestion Figure S2 of supplementary material
411 demonstrated that the addition of not only octanoate or glucose, but other growth
412 precursor such as pyruvate or fructose at equimolar concentration than octanoate,
413 avoided as well the long lag phase caused by the glycerol. These results strongly
414 suggested that the de-repression via GlpR and glycerol is also dependent on an active
415 metabolism (generation of ATP).

416 The finding that the long lag-phase of *P. putida* growing in glycerol can be
417 avoided either, by the addition of small amounts of some co-feeding substrates or by the
418 creation of a *glpR* knock-out mutant provides a great technological advance. Moreover,

in the case of the KT40GlpR mutant we have observed that PHA production improves not only due to less time invested in the process, but also to the best final yield when compared to the wild type strain.

Finally, our experiments suggest that *P. putida* has evolved a tightly regulated system for metabolizing a common substrate like glycerol. The prolonged lag-phase could prevent the development of the strain in a competitive habitat in the absence of other common substrates like glucose or fatty acids. However, the glycerol lag-phase can be considerably reduced when small amounts of some co-substrates are present in the medium. A similar effect has been also observed in the fluorescent pseudomonad strain R62 where the prolonged lag-phase in glycerol was reduced by the addition of less than 0.05% of succinate or citrate (Saharan *et al*, 2010). These authors observed that the GlpK activity increased about 15 times in the presence of the inducers. Though, acquiring a fine tuning of the glycerol regulatory system for a rapid response might depend on their respective environments.

Summing up, our findings have contributed not only to unravel the physiological causes of the long lag-phase produced by glycerol in the model strain *P. putida* KT2440 that hinders its use as carbon source for biotechnological applications, but they have also settled the bases for a rational design of an improved strain very useful for the efficient transformation of raw glycerol derived from the biodiesel industry not only into PHA but also into other valuable products.

Experimental procedures

Bacterial strains, media and growth conditions

Bacterial strains and plasmids used in this work are described in Table 4. *P.*

443 *putida* KT2440 genome complete nucleotide sequence is accessible in the data bank
444 (Nelson *et al.*, 2002). *E. coli* and *P. putida* strains were grown routinely for DNA
445 manipulations and for pre-cultures in lysogeny broth (LB) medium (Sambrook and
446 Russell, 2001; Bertani 2004) at 37°C and 30°C, respectively. The appropriate selection
447 antibiotics, gentamicin (10 μg/ml), chloramphenicol (34 μg/ml), ampicillin (100 μg/ml),
448 kanamycin (50 μg/ml), or tetracycline (5 μg/ml) were added when needed.

449 Standard growth experiments of *P. putida* were performed in M63 minimal
450 medium (13.6 g of KH_2PO_4/l, 2 g $(NH_4)_2SO_4$/l, 0.5 mg $FeSO_4 \cdot 7\ H_2O$/l, adjusted to pH
451 7.0 with KOH). For PHA production, *P. putida* strains were grown in 0.1 N M63
452 medium, which is a nitrogen-limited variation of the common M63 medium with only
453 0.2 g $(NH_4)_2SO_4$/l (ten times less ammonium) (Moldes *et al.*, 2004). These media were
454 supplemented with the appropriated carbon sources; the substrate concentrations were
455 chosen in order to use a carbon equimolar concentration for each of them. For the
456 standard growth experiments 20 mM glycerol, 7.5 mM octanoate, 10 mM glucose, 30
457 mM acetate, 20 mM pyruvate, 10 mM citrate, 15 mM succinate, 10 mM gluconate or 10
458 mM fructose were used as carbon sources. In the PHA production experiments an
459 excess of carbon source were used, this is 40 mM and 80 mM glycerol, 15 mM
460 octanoate or 20 mM glucose. Octanoate was assayed as inducer at 0.01 mM, 0.1 mM
461 and 1mM, glucose was also used as inducer at 1.33 mM (equimolar to 1mM). Pyruvate
462 (0.27 mM and 2.7 mM) and fructose (0.13 mM and 1.33 mM) were also assayed as
463 inducers (Fig. S2). All the medium components were purchased from Sigma-Aldrich
464 (St. Louis, MO, USA).

465 For *P. putida* growth experiments, LB pre-cultures cells were adjusted to an
466 optical density at 600 nm (OD600) of 0.3 in 0.1 N M63 plus the selected carbon source
467 or mixture of carbon sources. This culture process has been performed either in shake

flask or 96-microwell plates. Culture growth (200 ml) was monitored in shaking flasks (250 rpm) of 500 ml with a Shimadzu UV-260 spectrophotometer at 600 nm for 46 h. For the cultivation in 96-microwell plates, 200 µl aliquots were distributed in the microwells. The plates were incubated at 30°C for 46 h, with 20 seconds of heavy orbital shaking every 15 min using a Multiskan Ascent Incubator (Thermo Scientific, Waltham, MA, USA) that monitors optical density at 630 nm (OD_{630}) every 15 min. The growth curves shown are the average values from ≥6 replicates.

It is worth to notice that PHA content contributes considerably to cells turbidimetry, so the optical density gives mixed information about cell growth plus PHA accumulation and can only be used to determine the growth rates in absence of PHA. Growth rates have been calculated based on OD_{630} growth curves slope (h^{-1}) during the exponential growth period.

Construction of P. putida *KT2440 deletion mutants*

Standard molecular biology techniques were performed as previously described (Sambrook and Russell, 2001). The *glpR* and *hexR* genes, as well as the genomic region *phaC1ZC2*, were inactivated by allelic exchange homologous recombination using the mobilizable plasmid pK18*mob*sacB (Schäfer *et al*., 1994). The PCR primer pairs used for these constructions and the PCR fragments sizes originated are listed in Table 5; KT2440 genome was used as DNA template. PCR products were purified with the High Pure PCR product Purification Kit (Roche Applied Science, Basel, Switzerland) Each pair of two fragments were digested with the appropriate restriction enzymes (Takara Bio Inc., Shiga, Japan) and ligated using T4 DNA ligase (USB Corp., Affymetrix, Cleveland, OH, USA), resulting in the corresponding deleted version of each gene or genomic region. DNA fragments were purified with GeneClean Turbo kit (MP Biomedicals, Santa Ana, CA, USA). These deleted genes were cloned into the

corresponding unique sites of pK18*mob*sacB plasmid to yield the different plasmids listed in Table 4. Plasmid isolation was performed using High Pure Plasmid Isolation Kit (Roche Applied Science, Basel, Switzerland) and cloned inserts were confirmed by DNA sequencing by Secugen S.L. (Madrid, Spain). The resultant plasmids were used to deliver the different mutations to the host chromosome of each strain via homologous recombination. Triparental mating was performed following protocol described by Herrero *et al*. (1990), using *E. coli* DH10B as donor strain, *E. coli* HB101 pRK600 as helper strain and *P. putida* KT2440 (Table 4) as recipient strain. The strains resulted of this first recombination event were confirmed by PCR and the selected colonies were grown in LB during 6 hours and then plated on M63 10 mM citrate selective plates supplemented with 5% sucrose. Transconjugants sucrose resistant and kanamycin sensible were isolated and the second crossover event was confirmed by PCR. The resultant mutant strains were listed in Table 4.

Identification of transposon integration site in P. putida *KTH2 strain*

P. putida KTH2 genomic DNA was extracted using a standard procedure (Sambrook and Russell, 2001) and digested with *Not*I restriction enzyme (Takara Bio Inc., Shiga, Japan). The resulted fragments were cloned into *Not*I unique site of pUC18Not plasmid (Herrero *et al*., 1990), transformed in *E. coli* DH10B competent cells and plated on LB plates supplemented with ampicillin (pUC18Not plasmid selection marker) and kanamycin. Kanamycin resistant transconjugants imply that the fragment cloned into pUC18Not plasmid carries kanamycin resistance transposon fragment flanking the genomic region in which transposon where integrated. Plasmid isolation of the resultant pUC18Not derivative was performed using High Pure Plasmid Isolation Kit (Roche Applied Science, Basel, Switzerland) and cloned insert sequence was analyzed by DNA sequencing by Secugen S.L. (Madrid, Spain). Transposon

integration site in *P. putida* KTH2 strain was identified disrupting *aceA* (PP_4116) gene.

P. putida *KTH2* aceA *gene complementation*

The *aceA* coding sequence was amplified by PCR using aceA-5' and aceA-3' oligonucleotides listed in Table 5 and KT2442 genome as DNA template. The amplified DNA fragment was digested with *Hin*dIII and *Xba*I enzymes (Takara Bio Inc., Shiga, Japan) and then inserted into pIZ1016 vector (Moreno-Ruiz *et al*., 2003). The resulting pIZaceA recombinant plasmid was transformed into *E. coli* DH10B and then transferred by triparental mating (Herrero *et al*. 1990) to *P. putida* KT2442 and *P. putida* KTH2 strains.

Biomass calculation

It should be notice that PHA content disturbs cells turbidimetry, so the optical density cannot be used to estimate growth rates in terms of viable cells or biomass. Biomass concentrations, expressed in grams per litre, were determined gravimetrically. Briefly, culture medium (40 ml) was centrifuged for 30 min at 3800 *g* and 4ºC (centrifuge Sigma 3-18K, Osterode am Harz, Germany). Cell pellets were freeze-dried for 24 h in a VirTis Benchtop K Freeze Dryer (SP Industries, Gardiner, NY) and weighed.

GC analysis for PHA content determinations

Polyhydroxyalkanoate monomer composition and cellular PHA content were determined by GC of the methanolysed polyester. Methanolysis was carried out by suspending 5–10 mg of lyophilized cells in 2 ml of chloroform and 2 ml of methanol containing 15% sulphuric acid and 0.5 mg/ml of 3-methylbenzoic acid (internal standard), followed by an incubation at 100°C for 4 h. After cooling, 1 ml of

demineralised water was added and the organic phase containing the methyl esters was analysed by GC (Lageveen *et al.*, 1988; de Eugenio *et al.*, 2010a). A standard curve from 0.5 to 2mg of PHA (Biopolis S.L., Valencia, Spain) was used to interpolate sample data.

Glyceraldehyde-3-phosphate dehydrogenase (GAPDH) enzymatic assay

GAPDH enzymatic assay has been slightly modified from Pancholi and Fischetti (1992). Briefly, cells of *P. putida* strains were harvested by centrifugation (40ml culture) after 6 and 22 hours of culture and resuspended in GAPDH assay buffer pH 8.6 (50 mM Na_2HPO_4, 5 mM EDTA, 40 mM triethanolamine) plus 0.2 phenylmethylsulfonyl fluoride (PMSF). Cell debris was removed by 15 min centrifugation at 4ºC and 14000 g (centrifuge Sigma 1-15K, Osterode am Harz, Germany) and the clear supernatant was used as crude extract. The protein concentration was determined by the method of Bradford (Bradford, 1976), with bovine serum albumin as a standard. GAPDH activity was assayed at 30ºC by following NADH formation spectrophotometrically at 340 nm. The assay mixture contained GAPDH assay buffer supplemented with 2 mM cysteine (Tiwari and Campbell, 1969), 1 mM NAD, 2 mM glyceraldehyde 3-phosphate and 0.5 mg of protein extract.

Real Time quantitative Reverse Transcription PCR (qRT-PCR) assay

P. putida strains were cultivated overnight in LB medium, washed, resuspended in 0.1N M63 medium at 0.3 OD_{600} and incubated at 30ºC in shaking flasks (250 rpm) during 3 h with the correspondent substrate/s. After the incubation time aliquots of 50 ml were harvested by centrifugation at 4°C in tubes precooled on dry ice and quickly stored at −80 °C. The RNA samples were purified by using RNeasy Mini Kit (Qiagen, Düsseldorf, Germany). After proving the absence of contaminating DNA by polymerase

chain reaction (PCR), reverse transcription reactions for synthesis of total cDNA were carried out with 1 µg of RNA, 0.5 mM dNTPs, 200 U of SuperScript II Reverse Transcriptase (Invitrogen, Carlsbad, California, USA) and 2.5 µM of random hexamers as primers, in the buffer recommended by the manufacturer. Samples were initially heated at 65°C for 5 min and then incubated at 42°C for 2 h, terminated by incubation at 70°C for 15 min. The cDNA obtained was purified using Geneclean Turbo kit (MP Biomedicals, Santa Ana, CA, USA) and the concentration was measured using a NanoPhotometer™ Pearl (Implen, Munich, Germany). For the analysis of the transcripts levels target cDNAs (0.5 and 5 ng) and reference samples were amplified three times in separate PCR with 0.2 µM each of target primers and using iQ SYBR Green Supermix (Bio-Rad, Berkeley, California, USA) in a iQ5 Multicolor Real-Time PCR Detection System (Bio-Rad, Berkeley, California, USA). Target primers are listed in Table 5. Samples were initially denatured by heating at 95°C for 5 min, followed by 40 cycles of amplification (95°C, 30 s; test annealing temperature, 56°C, 30 s; elongation and signal acquisition, 72°C, 30 s). For quantification of the fluorescence values, a calibration curve was made using dilution series from 5.10^{-7} to 5 ng of *P. putida* KT2442 genomic DNA sample. cDNAs from the experimental samples were amplified using amounts within the linear range of the standard curve. After the PCR a melting curve was generated to confirm the amplification of a single product. Results were normalized relative to those obtained for the *rpoN* gene, as its expression is known to remain relatively constant throughout growth phase in both *E. coli* and *P. putida* (Jishage *et al*., 1996; Morales *et al.*, 2006; Yuste *et al*., 2006). qRT-PCR analyses were performed with RNA samples obtained from three independent biological replicas under identical conditions. A multifactorial analysis of variance (ANOVA) has been performed using Statgraphics software package (Statpoint

591 Technologies Inc., Warrenton, VA, USA) showing a statistical significance between the
592 six conditions analyzed (p = 0.0012for *glpF* gene and p = 0.0001 for *glpK* gene).

593

594 **Acknowledgments**

595 We are greatly indebted to Dr. Eduardo Diaz for helpful discussions. We thank
596 the technical works of A. Valencia and F. de la Peña. This work was supported by
597 grants from the Comisión Interministerial de Ciencia y Tecnología and CSIC
598 (BIO2010-21049 and 201120E092), and by the European Union Grant (NMP2-CT-
599 2007-026515). Isabel F. Escapa is a recipient of CSIC-I3P predoctoral fellowship.

600

601 **References**

602 Aparicio ML, Ruiz-Amil M, Vicente M, Cánovas JL (1971) The role of
603 phosphoglycerate kinase in the metabolism of *Pseudomonas putida*. FEBS Lett 14
604 (5):326-328.

605 Applebee MK, Joyce AR, Conrad TM, Pettigrew DW, Palsson BØ (2011)
606 Functional and metabolic effects of adaptive glycerol kinase (GLPK) mutants in
607 *Escherichia coli*. J Biol Chem 286 (26):23150-23159.

608 Ashby RD, Solaiman DKY, Foglia TA (2005) Synthesis of short-/medium-
609 chain-length poly(hydroxyalkanoate) blends by mixed culture fermentation of glycerol.
610 Biomacromolecules 6 (4):2106-2112.

611 Bagdasarian M, Lurz R, Rückert B, Franklin FC, Bagdasarian MM, Frey J,
612 Timmis KN (1981) Specific-purpose plasmid cloning vectors II. Broad host range, high
613 copy number, RSF1010-derived vectors, and a host-vector system for gene cloning in

614 *Pseudomonas*. Gene 16 (1-3):237-247.

615 Bertani G (2004) Lysogeny at mid-twentieth century: P1, P2, and other
616 experimental systems. J Bacteriol 186 (3):595-600.

617 Blevins WT, Feary TW, Phibbs PV (1975) 6-Phosphogluconate dehydratase
618 deficiency in pleiotropic carbohydrate-negative mutant strains of *Pseudomonas*
619 *aeruginosa*. J Bacteriol 121 (3):942-949.

620 Bormann EJ, Roth M (1999) The production of polyhydroxybutyrate by
621 *Methylobacterium rhodesianum* and *Ralstonia eutropha* in media containing glycerol
622 and casein hydrolysates. Biotechnol Lett 21 (12):1059-1063.

623 Bradford MM (1976) A rapid and sensitive method for the quantitation of
624 microgram quantities of protein utilizing the principle of protein-dye binding. Anal
625 Biochem 72:248-254.

626 Browne P, Barret M, O'Gara F, Morrissey JP (2010) Computational prediction
627 of the Crc regulon identifies genus-wide and species-specific targets of catabolite
628 repression control in *Pseudomonas* bacteria. BMC Microbiol 10 (1):300.

629 Castilho LR, Mitchell Da, Freire DMG (2009) Production of
630 polyhydroxyalkanoates (PHAs) from waste materials and by-products by submerged
631 and solid-state fermentation. Bioresour Technol 100 (23):5996-6009.

632 Cavalheiro JMBT, de Almeida MCMD, Grandfils C, da Fonseca MMR (2009)
633 Poly(3-hydroxybutyrate) production by *Cupriavidus necator* using waste glycerol.
634 Process Biochem 44 (5):509-515.

635 Cuskey SM, Phibbs PV (1985) Chromosomal mapping of mutations affecting
636 glycerol and glucose catabolism in *Pseudomonas aeruginosa* PAO. J Bacteriol 162
637 (3):872-880.

638 Chen GQ (2009) A microbial polyhydroxyalkanoates (PHA) based bio- and
639 materials industry. Chem Soc Rev 38 (8):2434-2446.

640 da Silva GP, Mack M, Contiero J (2009) Glycerol: A promising and abundant
641 carbon source for industrial microbiology. Biotechnol Adv 27 (1):30-39.

642 Daddaoua A, Krell T, Ramos JL (2009) Regulation of glucose metabolism in
643 *Pseudomonas*: the phosphorylative branch and Entner-Doudoroff enzymes are regulated
644 by a repressor containing a sugar isomerase domain. J Biol Chem 284 (32):21360-
645 21368.

646 de Almeida A, Giordano AM, Nikel PI, Pettinari MJ (2010) Effects of aeration
647 on the synthesis of poly(3-hydroxybutyrate) from glycerol and glucose in recombinant
648 *Escherichia coli*. Appl Environ Microbiol 76 (6):2036-2040.

649 de Eugenio LI, Escapa IF, Morales V, Dinjaski N, Galán B, García JL, Prieto
650 MA (2010a) The turnover of medium-chain-length polyhydroxyalkanoates in
651 *Pseudomonas putida* KT2442 and the fundamental role of PhaZ depolymerase for the
652 metabolic balance. Environ Microbiol 12 (1):207-221.

653 de Eugenio LI, Galán B, Escapa IF, Maestro B, Sanz JM, García JL, Prieto MA
654 (2010b) The PhaD regulator controls the simultaneous expression of the pha genes
655 involved in polyhydroxyalkanoate metabolism and turnover in *Pseudomonas putida*
656 KT2442. Environ Microbiol 12 (6):1591-1603.

657 de Riel JK, Paulus H (1978) Subunit dissociation in the allosteric regulation of
658 glycerol kinase from *Escherichia coli*. 1. Kinetic evidence. Biochemistry 17 (24):5134-
659 5140.

660 del Castillo T, Duque E, Ramos JL (2008) A set of activators and repressors
661 control peripheral glucose pathways in *Pseudomonas putida* to yield a common central

662 intermediate. J Bacteriol 190 (7):2331-2339.

663 Elbahloul Y, Steinbüchel A (2009) Large-scale production of poly(3-
664 hydroxyoctanoic acid) by *Pseudomonas putida* GPo1 and a simplified downstream
665 process. Appl Environ Microbiol 75 (3):643-651.

666 Escapa IF, Morales V, Martino VP, Pollet E, Averous L, García JL, Prieto MA
667 (2011) Disruption of beta-oxidation pathway in *Pseudomonas putida* KT2442 to
668 produce new functionalized PHAs with thioester groups. Appl Microbiol Biotechnol 89
669 (5):1583-1598.

670 Follonier S, Panke S, Zinn M (2011) A reduction in growth rate of *Pseudomonas*
671 *putida* KT2442 counteracts productivity advances in medium-chain-length
672 polyhydroxyalkanoate production from gluconate. Microb Cell Fact 10 (1):25.

673 Fonseca MP (2011) Búsqueda y caracterización de nuevos factores implicados
674 en represión catabólica en *Pseudomonas putida*. Ph.D. thesis, Universidad Autónoma,
675 Madrid.

676 Franklin FC, Bagdasarian M, Bagdasarian MM, Timmis KN (1981) Molecular
677 and functional analysis of the TOL plasmid pWWO from *Pseudomonas putida* and
678 cloning of genes for the entire regulated aromatic ring *meta* cleavage pathway. Proc
679 Natl Acad Sci U S A 78 (12):7458-7462.

680 Gao X, Chen JC, Wu Q, Chen GQ (2011) Polyhydroxyalkanoates as a source of
681 chemicals, polymers, and biofuels. Curr Opin Biotechnol 22:1-7.

682 Gomez JGC, Méndez BS, Nikel PI, Pettinari MJ, Prieto MA, Silva LF (2012)
683 Making green polymers even greener: Towards sustainable production of
684 polyhydroxyalkanoates from agroindustrial by-products. In: Petre M (ed) Advances in
685 Applied Biotechnology. InTech, Rijeka, Croatia, pp 41-62.

686 Heath HE, Gaudy ET (1978) Relationship between catabolism of glycerol and
687 metabolism of hexosephosphate derivatives by *Pseudomonas aeruginosa*. J Bacteriol
688 136 (2):638-646.

689 Herrero M, de Lorenzo V, Timmis KN (1990) Transposon vectors containing
690 non-antibiotic resistance selection markers for cloning and stable chromosomal
691 insertion of foreign genes in gram-negative bacteria. J Bacteriol 172 (11):6557-6567

692 Huijberts GN, Eggink G, de Waard P, Huisman GW, Witholt B (1992)
693 *Pseudomonas putida* KT2442 cultivated on glucose accumulates poly(3-
694 hydroxyalkanoates) consisting of saturated and unsaturated monomers. Appl Environ
695 Microbiol 58 (2):536-544.

696 Ibrahim MHA, Steinbüchel A (2009) Poly(3-hydroxybutyrate) production from
697 glycerol by *Zobellella denitrificans* MW1 *via* high-cell-density fed-batch fermentation
698 and simplified solvent extraction. Appl Environ Microbiol 75 (19):6222-6231.

699 Ibrahim MHA, Steinbüchel A (2010) *Zobellella denitrificans* strain MW1, a
700 newly isolated bacterium suitable for poly(3-hydroxybutyrate) production from
701 glycerol. J Appl Microbiol 108 (1):214-225.

702 Jishage M, Iwata A, Ueda S, Ishihama A (1996) Regulation of RNA polymerase
703 sigma subunit synthesis in *Escherichia coli*: intracellular levels of four species of sigma
704 subunit under various growth conditions. J Bacteriol 178 (18):5447-5451.

705 Johnson DT, Taconi KA (2009) The glycerin glut : Options for the value-added
706 conversion of crude glycerol resulting from biodiesel production. Environ Prog 26
707 (4):338-348.

708 Kawata Y, Aiba SI (2010) Poly(3-hydroxybutyrate) production by isolated
709 *Halomonas* sp. KM-1 using waste glycerol. Biosci Biotechnol Biochem 74 (1):175-177.

Kessler B, de Lorenzo V, Timmis KN (1992) A general system to integrate *lacZ* fusions into the chromosomes of gram-negative eubacteria: regulation of the *Pm* promoter of the *TOL* plasmid studied with all controlling elements in monocopy. Mol Gen Genet 233 (1-2):293-301.

Kim J, Jeon CO, Park W (2008) Dual regulation of *zwf-1* by both 2-keto-3-deoxy-6-phosphogluconate and oxidative stress in *Pseudomonas putida*. Microbiology 154 (Pt 12):3905-3916.

Kornberg HL (1966) The role and control of the glyoxylate cycle in Escherichia coli. The Biochemical journal 99 (1):1-11.

Kornberg HL, Krebs HA (1957) Synthesis of Cell Constituents from C2-Units by a Modified Tricarboxylic Acid Cycle. Nature 179 (4568):988-991.

Lageveen RG, Huisman GW, Preusting H, Ketelaar P, Eggink G, Witholt B (1988) Formation of polyesters by *Pseudomonas oleovorans*: effect of substrates on formation and composition of poly-(*R*)-3-hydroxyalkanoates and poly-(*R*)-3-hydroxyalkenoates. Appl Environ Microbiol 54 (12):2924-2932.

Lenz RW, Kim YB, Fuller RC (1992) Production of unusual bacterial polyesters by *Pseudomonas oleovorans* through cometabolism. FEMS Microbiol Lett 103 (2-4):207-214.

Luengo JM, García B, Sandoval A, Naharro G, Olivera ER (2003) Bioplastics from microorganisms. Curr Opin Microbiol 6 (3):251-260.

Madison LL, Huisman GW (1999) Metabolic engineering of poly(3-hydroxyalkanoates): from DNA to plastic. Microbiol Mol Biol Rev 63 (1):21-53.

Mahishi LH, Tripathi G, Rawal SK (2003) Poly(3-hydroxybutyrate) (PHB) synthesis by recombinant *Escherichia coli* harbouring *Streptomyces aureofaciens* PHB

734 biosynthesis genes: effect of various carbon and nitrogen sources. Microbiol Res 158
735 (1):19-27.

736 Martínez V, García P, García JL, Prieto MA (2011) Controlled autolysis
737 facilitates the polyhydroxyalkanoate recovery in *Pseudomonas putida* KT2440. Microb
738 Biotechnol 4 (4):533-547.

739 McCowen SM, Phibbs PV, Feary TW (1981) Glycerol catabolism in wild-type
740 and mutant strains of *Pseudomonas aeruginosa*. Curr Microbiol 5 (3):191-196.

741 Moldes C, Garcia P, Garcia JL, Prieto MA (2004) In vivo immobilization of
742 fusion proteins on bioplastics by the novel tag BioF. Appl Environ Microbiol 70
743 (6):3205-3212.

744 Morales G, Ugidos A, Rojo F (2006) Inactivation of the *Pseudomonas putida*
745 cytochrome o ubiquinol oxidase leads to a significant change in the transcriptome and to
746 increased expression of the CIO and *cbb3*-1 terminal oxidases. Environ Microbiol 8
747 (10):1764-1774.

748 Moreno-Ruiz E, Hernáez MJ, Martínez-Pérez O, Santero E (2003) Identification
749 and functional characterization of *Sphingomonas macrogolitabida* strain TFA genes
750 involved in the first two steps of the tetralin catabolic pathway. J Bacteriol 185
751 (6):2026-2030.

752 Moreno R, Martínez-Gomariz M, Yuste L, Gil C, Rojo F (2009) The
753 *Pseudomonas putida* Crc global regulator controls the hierarchical assimilation of
754 amino acids in a complete medium: evidence from proteomic and genomic analyses.
755 Proteomics 9 (11):2910-2928.

756 Nelson KE, Weinel C, Paulsen IT, Dodson RJ, Hilbert H, Martins dos Santos
757 VA, *et al.* (2002) Complete genome sequence and comparative analysis of the

758 metabolically versatile *Pseudomonas putida* KT2440. Environ Microbiol 4 (12):799-
759 808.

760 Nikel PI, Pettinari MJ, Galvagno MA, Méndez BS (2008) Poly(3-
761 hydroxybutyrate) synthesis from glycerol by a recombinant *Escherichia coli arcA*
762 mutant in fed-batch microaerobic cultures. Appl Microbiol Biotechnol 77 (6):1337-
763 1343.

764 Novotny MJ, Frederickson WL, Waygood EB, Saier MH (1985) Allosteric
765 regulation of glycerol kinase by enzyme IIIglc of the phosphotransferase system in
766 *Escherichia coli* and *Salmonella typhimurium*. J Bacteriol 162 (2):810-816.

767 Pachauri N, He B (2006) Value-added utilization of crude glycerol from
768 biodiesel production: a survey of current research activities. Paper presented at the
769 Encontro Internacional Anual da American Society of Agricultural and Biological
770 Engineers, University of Idaho, Moscow.

771 Pancholi V, Fischetti VA (1992) A major surface protein on group A
772 streptococci is a glyceraldehyde-3-phosphate-dehydrogenase with multiple binding
773 activity. J Exp Med 176 (2):415-426.

774 Prieto MA, de Eugenio LI, Galán B, Luengo JM, Witholt B (2007) Synthesis
775 and degradation of polyhydroxyalkanoates. In: Ramos JL, Filloux A (eds)
776 Pseudomonas: a Model System in Biology, vol V. Pseudomonas vol V. Springer,
777 Berlin, Germany, pp 397-428.

778 Prieto MA, Díaz E, García JL (1996) Molecular characterization of the 4-
779 hydroxyphenylacetate catabolic pathway of *Escherichia coli* W: engineering a mobile
780 aromatic degradative cluster. J Bacteriol 178 (1):111-120.

781 Reddy SV, Thirumala M, Mahmood SK (2009) A novel *Bacillus* sp.

782 accumulating poly (3-hydroxybutyrate-co-3-hydroxyvalerate) from a single carbon
783 substrate. J Ind Microbiol Biotechnol 36 (6):837-843.

784 Rehm BH (2010) Bacterial polymers: biosynthesis, modifications and
785 applications. Nat Rev Microbiol 8 (8):578-592.

786 Rojo F (2010) Carbon catabolite repression in *Pseudomonas*: optimizing
787 metabolic versatility and interactions with the environment. FEMS Microbiol Rev 34
788 (5):658-684.

789 Saharan K, Sarma MVRK, Roesti AS, Prakash A, Johri BN, Aragno M, Bisaria
790 VS, Sahai V, Conditions AB (2010) Cell Growth and Metabolites Produced by
791 Fluorescent Pseudomonad R62 in Modified Chemically Defined Medium. World
792 Academy of Science, Engineering and Technology:867-871.

793 Sambrook J, Russell DW (2001) Molecular cloning: a laboratory manual. Cold
794 Spring Harbor Laboratory Press, Cold Spring Harbor, NY.

795 Schäfer A, Tauch A, Jäger W, Kalinowski J, Thierbach G, Pühler A (1994)
796 Small mobilizable multi-purpose cloning vectors derived from the *Escherichia coli*
797 plasmids pK18 and pK19: selection of defined deletions in the chromosome of
798 *Corynebacterium glutamicum*. Gene 145 (1):69-73.

799 Schweizer HP, Jump R, Po C (1997) Structure and gene-polypeptide
800 relationships of the region encoding glycerol diffusion facilitator (*glpF*) and glycerol
801 kinase (*glpK*) of *Pseudomonas aeruginosa*. Microbiology 143:1287-1297.

802 Schweizer HP, Po C (1994) Cloning and nucleotide sequence of the *glpD* gene
803 encoding *sn*-glycerol-3-phosphate dehydrogenase of *Pseudomonas aeruginosa*. J
804 Bacteriol 176 (8):2184-2193.

805 Schweizer HP, Po C (1996) Regulation of glycerol metabolism in *Pseudomonas*

806 *aeruginosa*: characterization of the *glpR* repressor gene. J Bacteriol 178 (17):5215-
807 5221.

808 Serafim LS, Lemos PC, Albuquerque MGE, Reis MAM (2008) Strategies for
809 PHA production by mixed cultures and renewable waste materials. Appl Microbiol
810 Biotechnol 81 (4):615-628.

811 Solaiman DKY, Ashby RD, Foglia Ta, Marmer WN (2006) Conversion of
812 agricultural feedstock and coproducts into poly(hydroxyalkanoates). Appl Microbiol
813 Biotechnol 71 (6):783-789.

814 Sun Z, Ramsay JA, Guay M, Ramsay BA (2007) Fermentation process
815 development for the production of medium-chain-length poly-3-hyroxyalkanoates. Appl
816 Microbiol Biotechnol 75 (3):475-485.

817 Tiwari NP, Campbell JJ (1969) Enzymatic control of the metabolic activity of
818 *Pseudomonas aeruginosa* grown in glucose or succinate media. Biochim Biophys Acta
819 192 (3):395-401.

820 Velázquez F, Pflüger K, Cases I, de Eugenio LI, de Lorenzo V (2007) The
821 phosphotransferase system formed by PtsP, PtsO, and PtsN proteins controls production
822 of polyhydroxyalkanoates in *Pseudomonas putida*. J Bacteriol 189 (12):4529-4533.

823 Vicente M, Cánovas JL (1973) Regulation of the glucolytic enzymes in
824 *Pseudomonas putida*. Arch Mikrobiol 93 (1):53-64.

825 Wang Q, Nomura CT (2010) Monitoring differences in gene expression levels
826 and polyhydroxyalkanoate (PHA) production in *Pseudomonas putida* KT2440 grown on
827 different carbon sources. J Biosci Bioeng 110 (6):653-659.

828 Williams SG, Greenwood JA, Jones CW (1994) The effect of nutrient limitation
829 on glycerol uptake and metabolism in continuous cultures of *Pseudomonas aeruginosa*.

Microbiology 140 (11):2961-2969.

Yuste L, Hervás AB, Canosa I, Tobes R, Jiménez JI, Nogales J, Pérez-Pérez MM, Santero E, Díaz E, Ramos JL, de Lorenzo V, Rojo F (2006) Growth phase-dependent expression of the *Pseudomonas putida* KT2440 transcriptional machinery analysed with a genome-wide DNA microarray. Environ Microbiol 8 (1):165-177.

Zeng G, Ye S, Larson TJ (1996) Repressor for the *sn*-glycerol 3-phosphate regulon of *Escherichia coli* K-12: primary structure and identification of the DNA-binding domain. J Bacteriol 178 (24):7080-7089.

Zinn M, Witholt B, Egli T (2001) Occurrence, synthesis and medical application of bacterial polyhydroxyalkanoate. Adv Drug Delivery Rev 53 (1):5-21.

Zwaig N, Kistler WS, Lin EC (1970) Glycerol kinase, the pacemaker for the dissimilation of glycerol in *Escherichia coli*. J Bacteriol 102 (3):753-759.

Zwaig N, Lin EC (1966) Feedback inhibition of glycerol kinase, a catabolic enzyme in *Escherichia coli*. Science (New York, NY) 153 (3737):755-757.

Figure legends

Figure 1. Scheme of glycerol and carbohydrates biochemical pathways in *P. putida* KT2440 based on genome annotation and the works by Schweizer and Po (1996), del Castillo *et al*. (2008), and Kim *et al*. (2008). Gene names and identification numbers as annotated in the genome data bank (KEGG Pathway Database: http://www.genome.jp/kegg/pathway.html) are shown. Genes enclosed in dark green boxes are under the control of the GlpR transcriptional regulator, whose inducer is glycerol-3-P (G3P) (light green box) (Schweizer and Po, 1996). Genes enclosed in blue boxes are under the control of the HexR transcriptional regulator directly (dark blue), or indirectly through GltR2/GltS two component system (cyan) (del Castillo *et al*., 2008). 2-keto-3-deoxy-6-P-gluconate (KDPG) (light blue box) has been proposed to be HexR inducer (Daddaoua *et al*., 2009). Gene names highlighted in red color identified genes bearing a Crc (catabolite repression control regulatory protein) binding motif (Browne *et al*., 2010). *oprB-1,* outer-membrane porin; *gtsABCD*, sugar ABC transporter; *glk*, glucokinase; *zwf-1*, glucose 6-P dehydrogenase; *pgl*, 6-phosphogluconolactonase; *edd*, 6-phosphogluconate dehydratase; *eda*, 2-dehydro-3-deoxyphosphogluconate aldolase; *gap-1*, glyceraldehyde-3-phosphate dehydrogenase (GAPDH); *glpF*, glycerol facilitator; *glpK*, glycerol kinase; *glpD*, G3P dehydrogenase.

Figure 2. OD_{630} turbidimetric profiles of *P. putida* KT2440 cells growing in M63 media using different substrates as carbon sources. The represented values are the average ($n \geq 6$) of the OD_{630} data obtained from the 96-microwell experiments.

Figure 3. Fatty acid based co-feeding strategies for stimulation of glycerol growth *versus* PHA accumulation **A.** OD_{630} turbidimetric profiles of *P. putida* KT2440 cells growing in M63 0.1N media using 40 mM glycerol (black circles), 15 mM

octanoate (white circles) or 40 mM glycerol plus different octanoate concentrations (grey symbols) as carbon sources. **B.** OD_{630} turbidimetric profiles of *P. putida* KT40C1ZC2 cells growing in M63 0.1N media using 40 mM glycerol (black circles), 15 mM octanoate (white circles) or 40 mM glycerol plus different octanoate concentrations (grey symbols) as carbon sources. The represented values are the average ($n \geq 6$) of the OD_{630} data obtained from the 96-microwell experiments.

Figure 4. Fatty acid based co-feeding strategies for stimulation of glycerol growth *versus* TCA cycle functionality **A.** OD_{630} turbidimetric profiles of *P. putida* KT2442 (circles) and *P. putida* KTH2 (triangles) cells growing in M63 0.1N media using 40 mM glycerol (black symbols), 15 mM octanoate (white symbols) or 40 mM glycerol plus 1 mM octanoate (grey symbols) as carbon sources. **B.** OD_{630} turbidimetric profiles of *P. putida* KT2442 (pIZaceA) (circles) and *P. putida* KTH2 (pIZaceA) (triangles) cells growing in M63 0.1N media using 40 mM glycerol (black symbols), 15 mM octanoate (white symbols) or 40 mM glycerol plus 1 mM octanoate (grey symbols) as carbon sources. The represented values are the average ($n \geq 6$) of the OD_{630} data obtained from the 96-microwell experiments. **C.** PHA content (% of the total CDW) of *P. putida* KT2442 and *P. putida* KTH2 cells growing in M63 0.1N media using 40 mM glycerol (black bars), 15 mM octanoate (white bars) or 40 mM glycerol plus 1 mM octanoate (grey bars) as carbon sources. The results corresponding to one experiment are shown, and values where reproducible in three separate experiments, with standard deviations of < 10%.

Figure 5. A. Evaluation of glycerol growth stimulation, biomass and PHA production in the strain *P. putida* KT2440. OD_{630} turbidimetric profiles of *P. putida* KT2440 cells growing in microtitter plates in M63 0.1N media using 40 mM glycerol (black circles), 15 mM octanoate (white triangles), 40 mM glycerol plus 1 mM

897 octanoate (grey triangles), 20 mM glucose (white squares) or 40 mM glycerol plus 1.3
898 mM glucose (grey squares) as carbon sources. The represented values are the average (n
899 ≥ 6) of the OD_{630} data obtained from the 96-microwell experiments. **B.** OD_{600}
900 turbidimetric profiles of *P. putida* KT2440 cells growing in shaking flasks in M63 0.1N
901 media using 40 mM glycerol (black circles), 15 mM octanoate (white triangles), 40 mM
902 glycerol plus 1 mM octanoate (grey triangles), 20 mM glucose (white squares) or 40
903 mM glycerol plus 1.3 mM glucose (grey squares) as carbon sources. Media and
904 standard deviation of three independent flask culture experiments are shown. ↓ indicates
905 times of cultivation in which samples were taken for GADPH enzymatic assays. ⇣
906 indicates times of cultivation in which samples were taken for biomass and PHA
907 content determination assays. **C.** Biomass and PHA content (mg/ml) of panel B
908 cultures.

909 **Figure 6.** Glycerol growth stimulation by inactivation of the transcriptional
910 regulator GlpR. OD_{630} turbidimetric profiles in M63 0.1N media of *P. putida* KT2440
911 cells using 40 mM glycerol (black circles) or 40 mM glycerol plus 1.3 mM glucose
912 (black triangles) as carbon sources and *P. putida* KT2440 mutant strains using 40 mM
913 glycerol (KT40GlpR, white triangles; KT40HexR, grey circles; KT40HexR-GlpR, grey
914 triangles; KTCRC, white circles). The represented values are the average (n≥ 6) of the
915 OD_{630} data obtained from the 96-microwell experiments.

916 **Figure 7.** Transcriptional analysis by qRT-PCR of *glpF* and *glpK* genes in *P.*
917 *putida* KT2440 (solid bars) and GlpR minus strains (striped bars). **A.** Genetic
918 organization of *glp* cluster in *P. putida* KT2440 based on genome data bank annotation
919 (KEGG Pathway Database: http://www.genome.jp/kegg/pathway.html) and *P.*
920 *aeruginosa glp* cluster analysis (Schweizer and Po, 1996). *glpF*, glycerol facilitator;
921 *glpK*, glycerol kinase; *glpD*, G3P dehydrogenase; *glpR*, glycerol transcriptional

regulator. **B.** Transcriptional analysis by qRT-PCR of *glpF* gene. **C.** Transcriptional analysis by qRT-PCR of *glpK* gene. Media and standard error from three independent biological replicas are shown. Grey bars indicate cells growing in 40 mM glycerol; white bars indicate cells growing in 15mM octanoate; black bars indicate cells growing in 40 mM glycerol plus 1 mM octanoate as inducer.

Figure 8. Evaluation of glycerol growth stimulation, biomass and PHA production in the strain *P. putida* KT40GlpR **A.** OD_{630} turbidimetric profiles of *P. putida* KT40GlpR cells growing in microtitter plates in M63 0.1N media using 40 mM glycerol (black circles), 15 mM octanoate (white triangles), 40 mM glycerol plus 1 mM octanoate (grey triangles), 20 mM glucose (white squares) or 40 mM glycerol plus 1.3 mM glucose (grey squares) as carbon sources. The represented values are the average ($n \geq 6$) of the OD_{630} data obtained from the 96-microwell experiments. **B.** OD_{600} turbidimetric profiles of *P. putida* KT40GlpR cells growing in shaking flasks in M63 0.1N media using 40 mM glycerol (black circles), 15 mM octanoate (white triangles), 40 mM glycerol plus 1 mM octanoate (grey triangles), 20 mM glucose (white squares) or 40 mM glycerol plus 1.3 mM glucose (grey squares) as carbon sources. Media and standard deviation of three independent flask culture experiments are shown. ↓ indicates times of cultivation in which samples were taken for GADPH enzymatic assays. ⇣ indicates times of cultivation in which samples were taken for biomass and PHA content determination assays. **C.** Biomass and PHA content (mg/ml) of panel B cultures.

Figure S1. Monomer composition of PHA polymer accumulated by *P. putida* KT2440 (panels A and B) and KT40GlpR (panels C and D) cultures analyzed in Figure 5B and 8B. Media of three independent flask culture experiments are shown with standard deviations of <10%. OH-C6, 3-hydroxyhexanoate; OH-C8, 3-

947 hydroxyoctanoate; OH-C10, 3-hydroxydecanoate; OH-C12, 3-hydroxydodecanoate;
948 OH-C12:1, 3-hydroxy-5-cis-dodecenoate.

949 **Figure S2.** OD_{630} turbidimetric profiles of *P. putida* KT2440 cells growing in
950 M63 media using 20 mM glycerol (black circles) or 20 mM glycerol plus different
951 pyruvate (**A**) and fructose (**B**) concentrations (grey symbols) as carbon sources. The
952 represented values are the average (n = 6) of the OD_{630} data obtained from the 96-
953 microwell experiments.

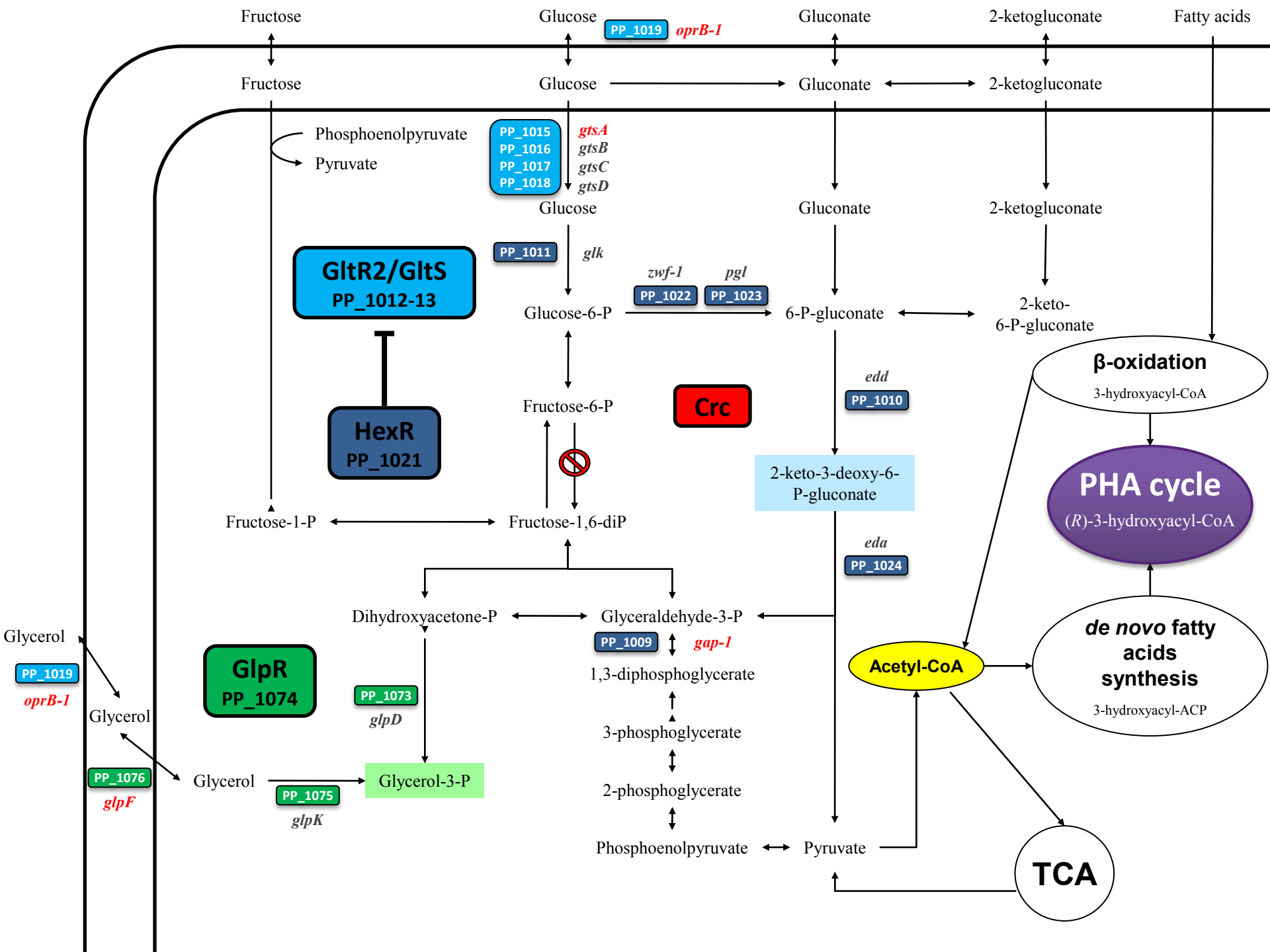
Fructose
Glucose
PP_1019
oprB-1
Gluconate
2-ketogluconate
Fatty acids
Fructose
Glucose
Gluconate
2-ketogluconate
Phosphoenolpyruvate
Pyruvate
PP_1015
PP_1016
PP_1017
PP_1018
gtsA
gtsB
gtsC
gtsD
Glucose
Gluconate
2-ketogluconate
PP_1011
glk
GltR2/GltS
PP_1012-13
zwf-1
pgl
PP_1022
PP_1023
Glucose-6-P
6-P-gluconate
2-keto-
6-P-gluconate
β-oxidation
3-hydroxyacyl-CoA
HexR
PP_1021
Crc
edd
PP_1010
Fructose-6-P
PHA cycle
(R)-3-hydroxyacyl-CoA
2-keto-3-deoxy-6-
P-gluconate
Fructose-1-P
Fructose-1,6-diP
eda
PP_1024
Dihydroxyacetone-P
Glyceraldehyde-3-P
PP_1009
gap-1
Glycerol
PP_1019
oprB-1
GlpR
PP_1074
Acetyl-CoA
de novo fatty
acids
synthesis
3-hydroxyacyl-ACP
PP_1073
glpD
1,3-diphosphoglycerate
Glycerol
3-phosphoglycerate
PP_1076
glpF
Glycerol
PP_1075
glpK
Glycerol-3-P
2-phosphoglycerate
Phosphoenolpyruvate
Pyruvate
TCA

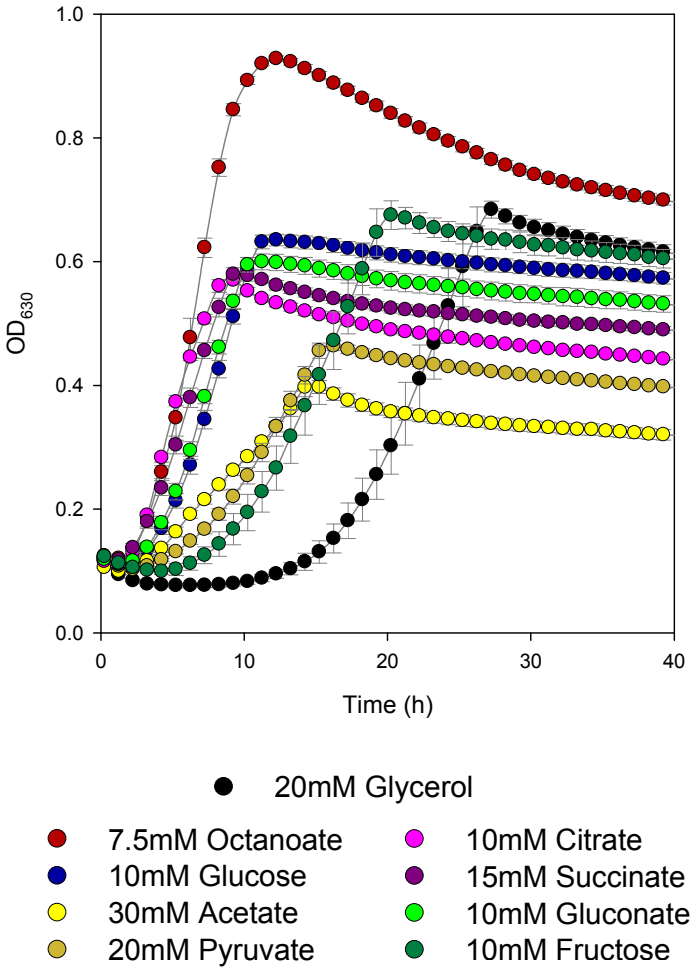
1.0
0.8
0.6
0.4
0.2
0.0
OD630
0
10
20
30
40
Time (h)
20mM Glycerol
7.5mM Octanoate
10mM Glucose
30mM Acetate
20mM Pyruvate
10mM Citrate
15mM Succinate
10mM Gluconate
10mM Fructose

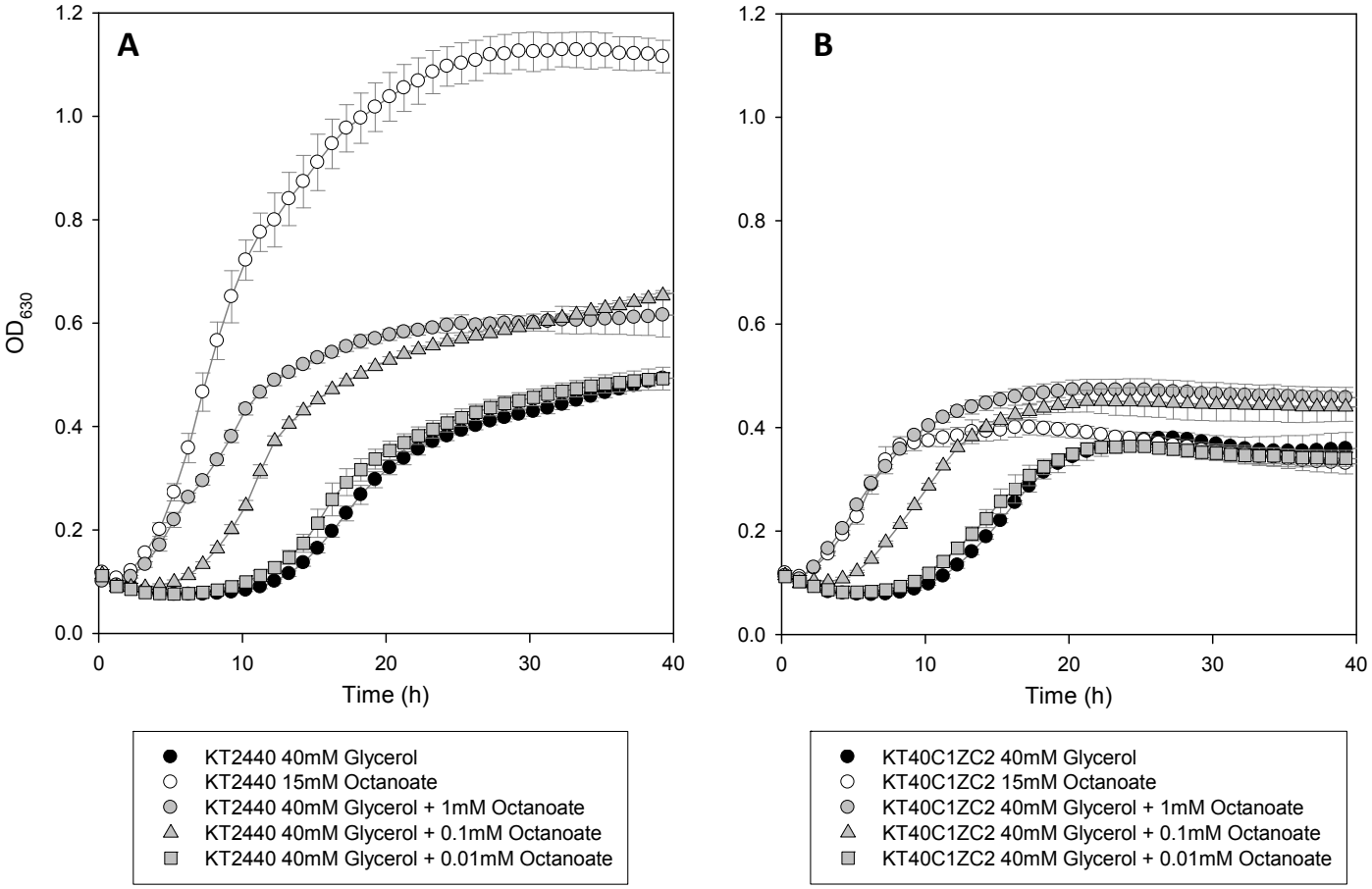
A
B
OD630
Time (h)
KT2440 40mM Glycerol
KT2440 15mM Octanoate
KT2440 40mM Glycerol + 1mM Octanoate
KT2440 40mM Glycerol + 0.1mM Octanoate
KT2440 40mM Glycerol + 0.01mM Octanoate
KT40C1ZC2 40mM Glycerol
KT40C1ZC2 15mM Octanoate
KT40C1ZC2 40mM Glycerol + 1mM Octanoate
KT40C1ZC2 40mM Glycerol + 0.1mM Octanoate
KT40C1ZC2 40mM Glycerol + 0.01mM Octanoate

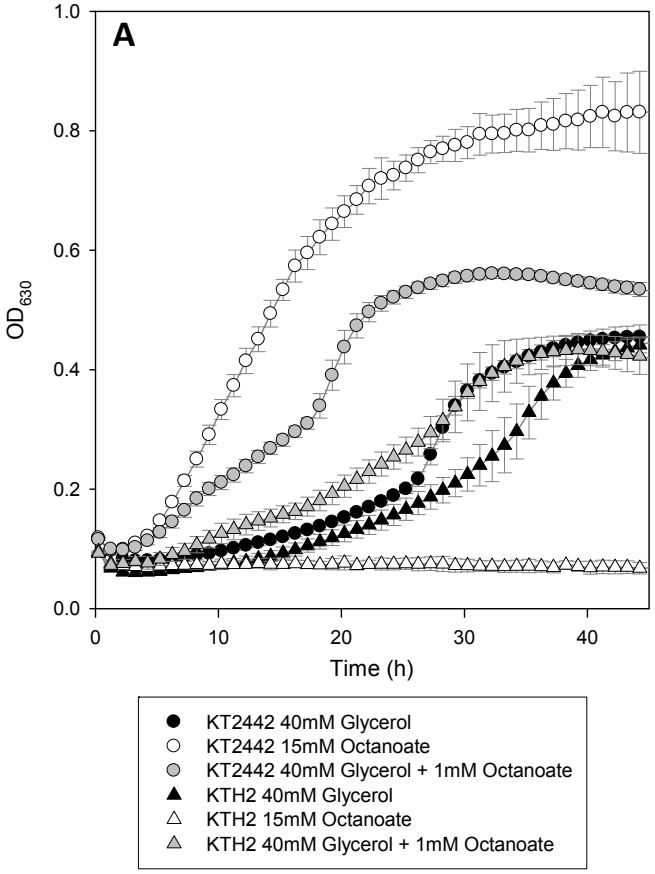
A
OD630
Time (h)
KT2442 40mM Glycerol
KT2442 15mM Octanoate
KT2442 40mM Glycerol + 1mM Octanoate
KTH2 40mM Glycerol
KTH2 15mM Octanoate
KTH2 40mM Glycerol + 1mM Octanoate

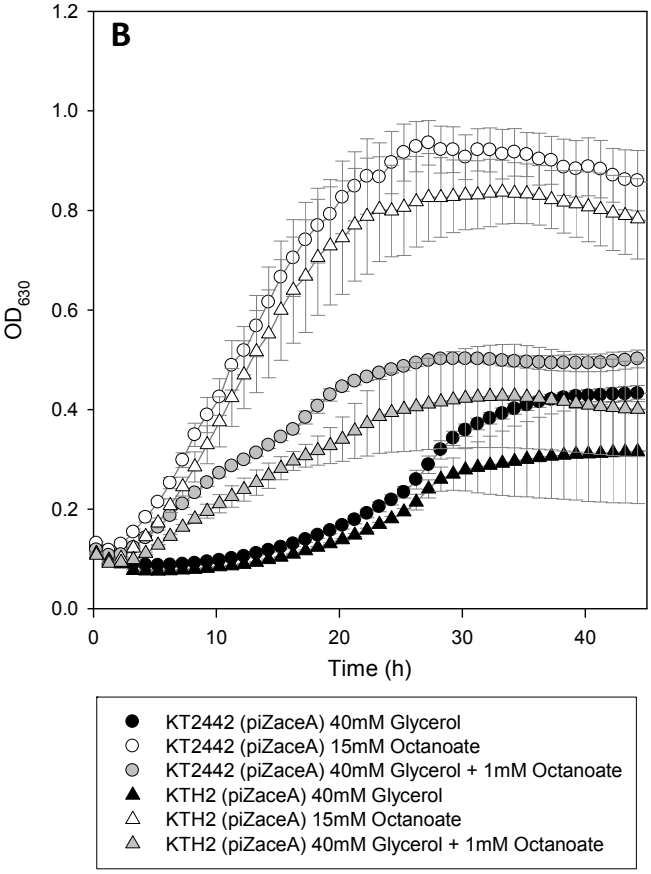
B
OD630
Time (h)
KT2442 (piZaceA) 40mM Glycerol
KT2442 (piZaceA) 15mM Octanoate
KT2442 (piZaceA) 40mM Glycerol + 1mM Octanoate
KTH2 (piZaceA) 40mM Glycerol
KTH2 (piZaceA) 15mM Octanoate
KTH2 (piZaceA) 40mM Glycerol + 1mM Octanoate

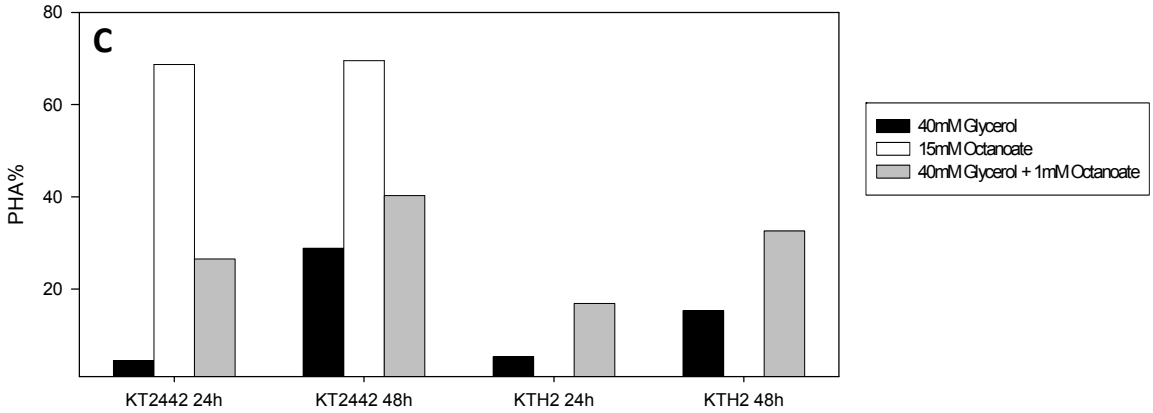
C
PHA%
KT2442 24h
KT2442 48h
KTH2 24h
KTH2 48h
40mM Glycerol
15mM Octanoate
40mM Glycerol + 1mM Octanoate

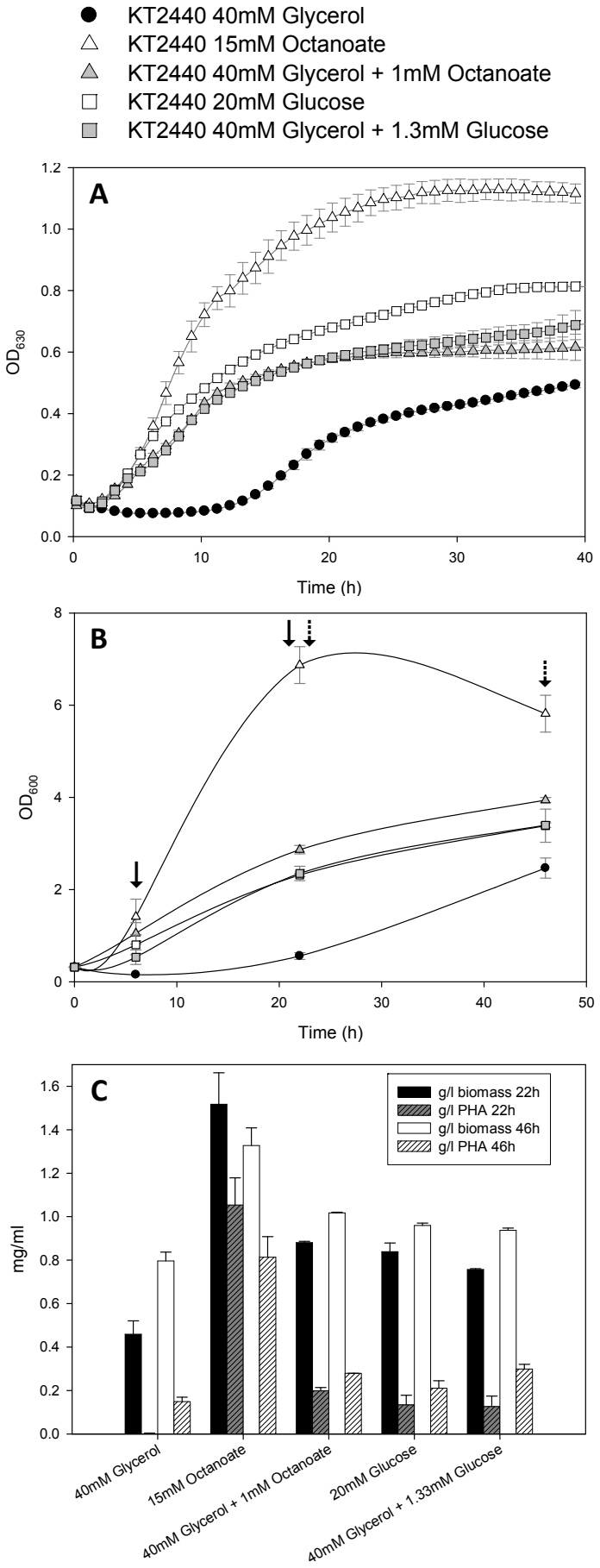
KT2440 40mM Glycerol
KT2440 15mM Octanoate
KT2440 40mM Glycerol + 1mM Octanoate
KT2440 20mM Glucose
KT2440 40mM Glycerol + 1.3mM Glucose
A
OD630
Time (h)
B
OD600
Time (h)
C
mg/ml
g/l biomass 22h
g/l PHA 22h
g/l biomass 46h
g/l PHA 46h
40mM Glycerol
15mM Octanoate
40mM Glycerol + 1mM Octanoate
20mM Glucose
40mM Glycerol + 1.33mM Glucose

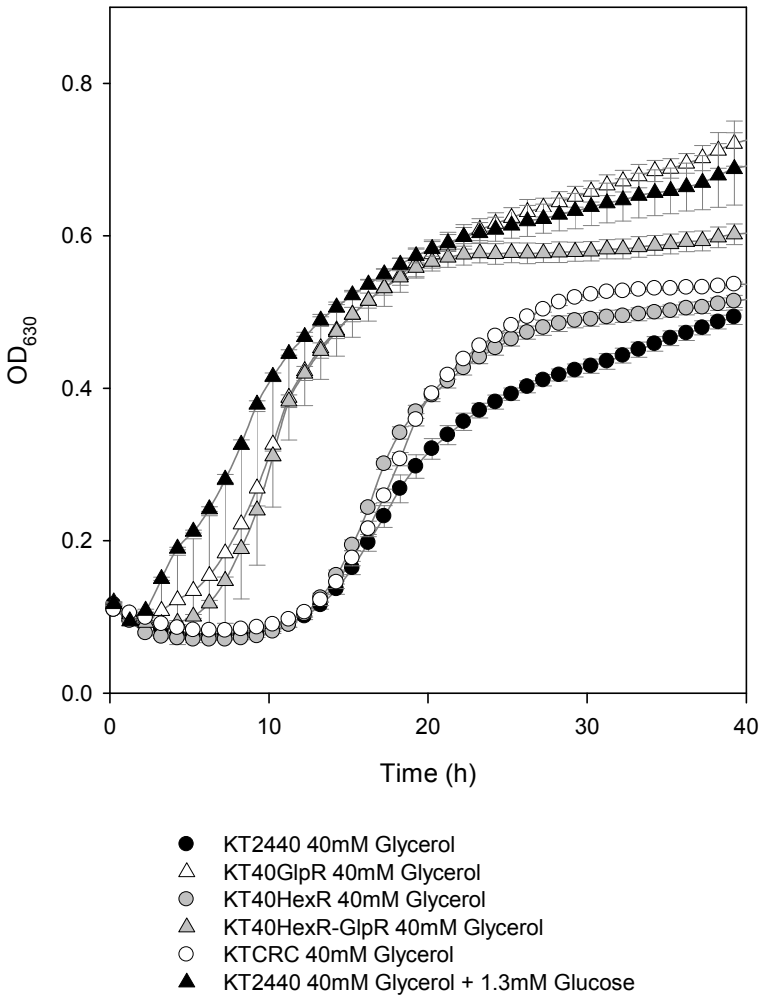
0.8
0.6
0.4
0.2
0.0
OD630
0
10
20
30
40
Time (h)
KT2440 40mM Glycerol
KT40GlpR 40mM Glycerol
KT40HexR 40mM Glycerol
KT40HexR-GlpR 40mM Glycerol
KTCRC 40mM Glycerol
KT2440 40mM Glycerol + 1.3mM Glucose

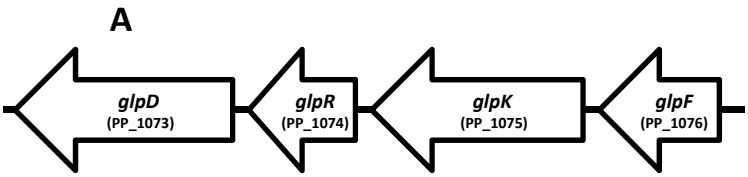
A
glpD
(PP_1073)
glpR
(PP_1074)
glpK
(PP_1075)
glpF
(PP_1076)

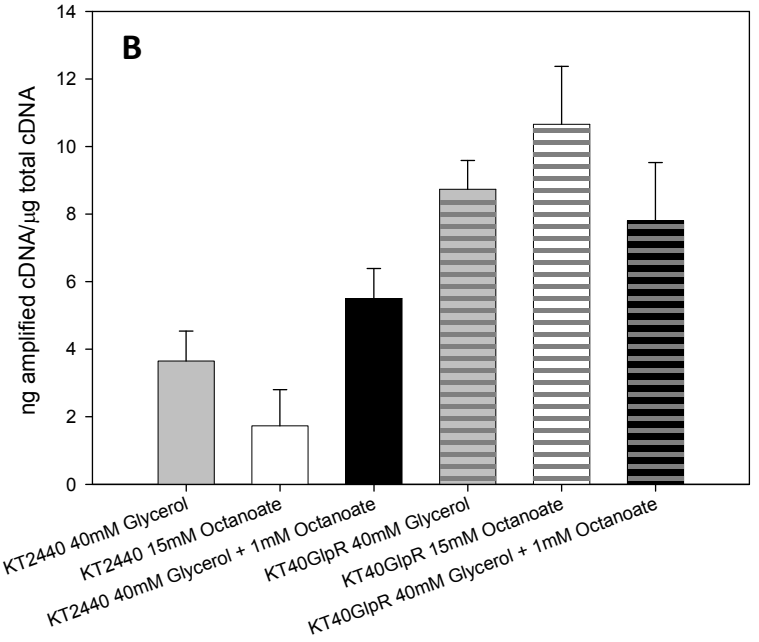
B
ng amplified cDNA/µg total cDNA
0
2
4
6
8
10
12
14
KT2440 40mM Glycerol
KT2440 15mM Octanoate
KT2440 40mM Glycerol + 1mM Octanoate
KT40GlpR 40mM Glycerol
KT40GlpR 15mM Octanoate
KT40GlpR 40mM Glycerol + 1mM Octanoate

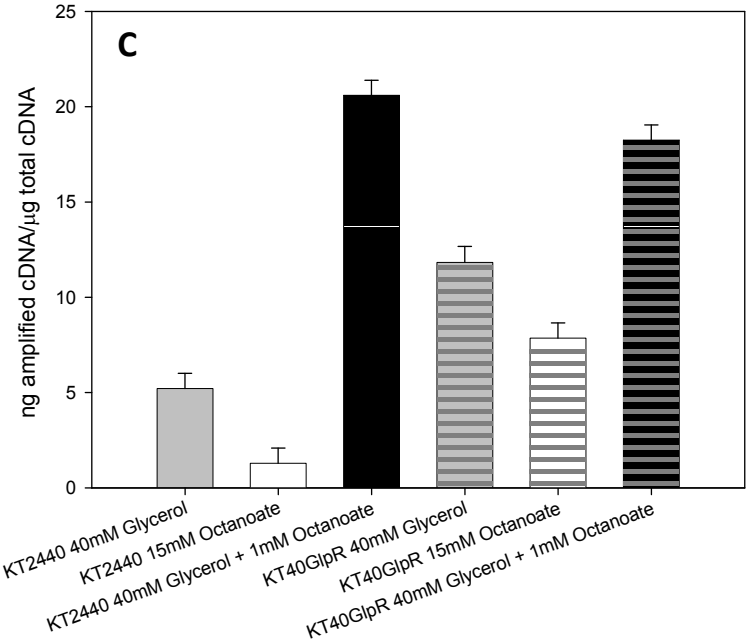
C
ng amplified cDNA/µg total cDNA
0
5
10
15
20
25
KT2440 40mM Glycerol
KT2440 15mM Octanoate
KT2440 40mM Glycerol + 1mM Octanoate
KT40GlpR 40mM Glycerol
KT40GlpR 15mM Octanoate
KT40GlpR 40mM Glycerol + 1mM Octanoate

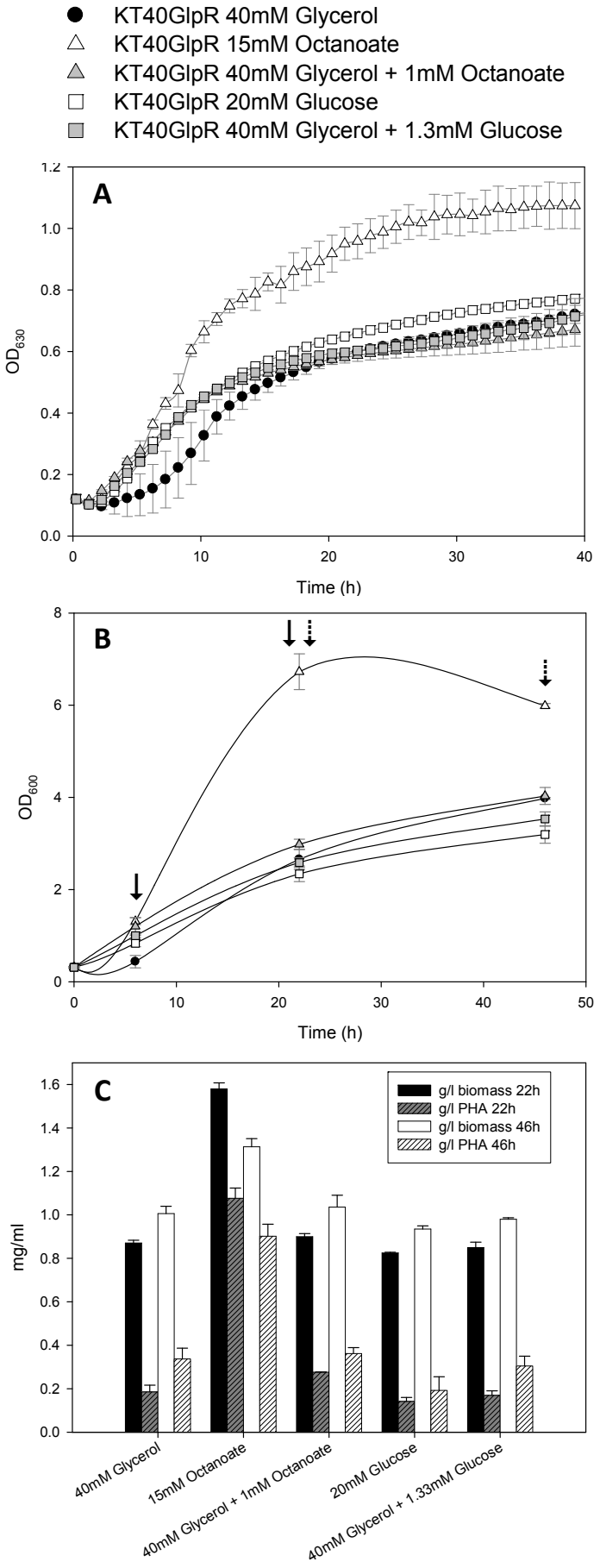
KT40GlpR 40mM Glycerol
KT40GlpR 15mM Octanoate
KT40GlpR 40mM Glycerol + 1mM Octanoate
KT40GlpR 20mM Glucose
KT40GlpR 40mM Glycerol + 1.3mM Glucose
A
OD630
Time (h)
B
OD600
Time (h)
C
g/l biomass 22h
g/l PHA 22h
g/l biomass 46h
g/l PHA 46h
mg/ml
40mM Glycerol
15mM Octanoate
40mM Glycerol + 1mM Octanoate
20mM Glucose
40mM Glycerol + 1.33mM Glucose

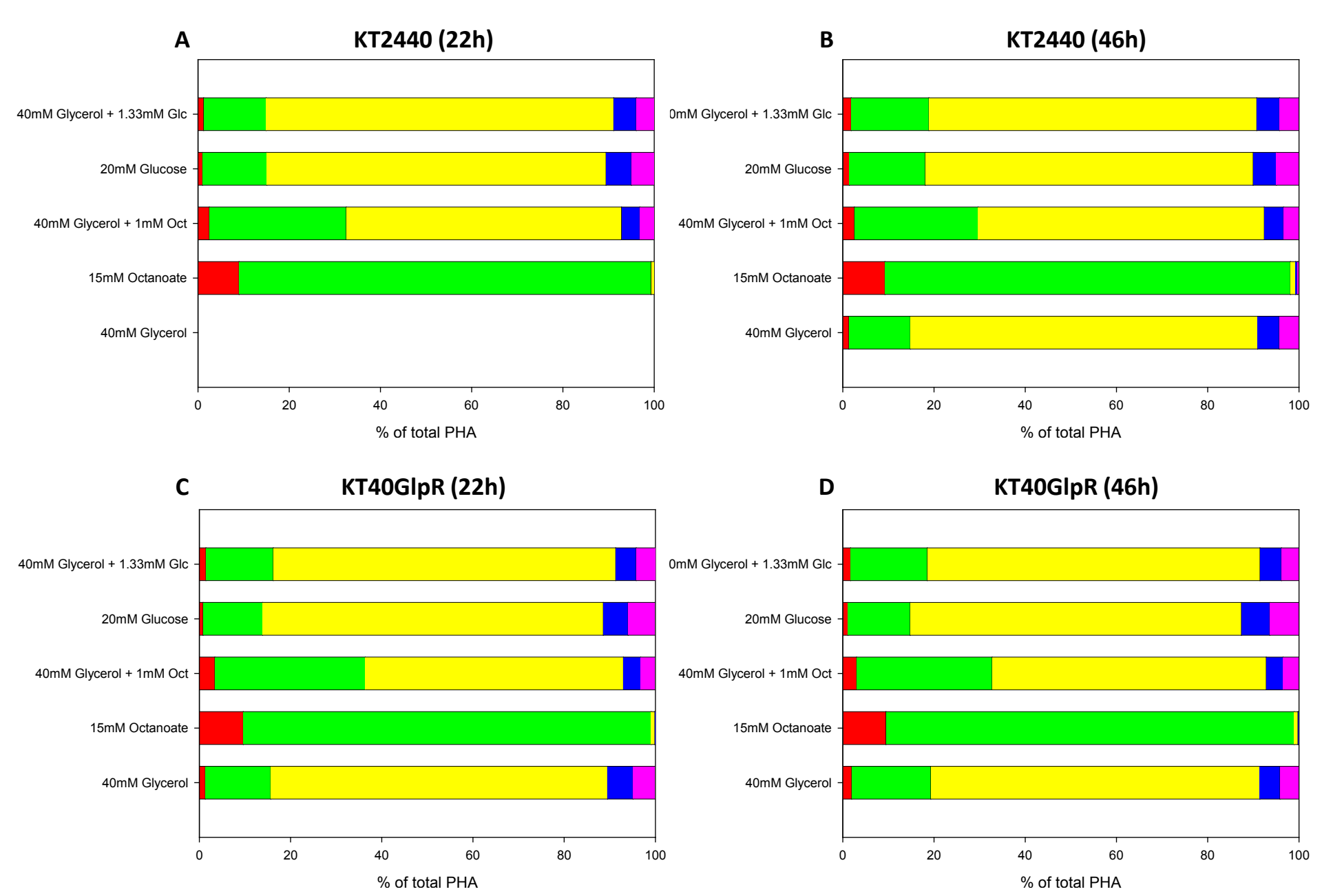
A
KT2440 (22h)
40mM Glycerol + 1.33mM Glc
20mM Glucose
40mM Glycerol + 1mM Oct
15mM Octanoate
40mM Glycerol
0
20
40
60
80
100
% of total PHA
B
KT2440 (46h)
0mM Glycerol + 1.33mM Glc
20mM Glucose
40mM Glycerol + 1mM Oct
15mM Octanoate
40mM Glycerol
0
20
40
60
80
100
% of total PHA
C
KT40GlpR (22h)
40mM Glycerol + 1.33mM Glc
20mM Glucose
40mM Glycerol + 1mM Oct
15mM Octanoate
40mM Glycerol
0
20
40
60
80
100
% of total PHA
D
KT40GlpR (46h)
0mM Glycerol + 1.33mM Glc
20mM Glucose
40mM Glycerol + 1mM Oct
15mM Octanoate
40mM Glycerol
0
20
40
60
80
100
% of total PHA
% OH-C6
% OH- C8
% OH- C10
% OH- C12
% OH- C12:1

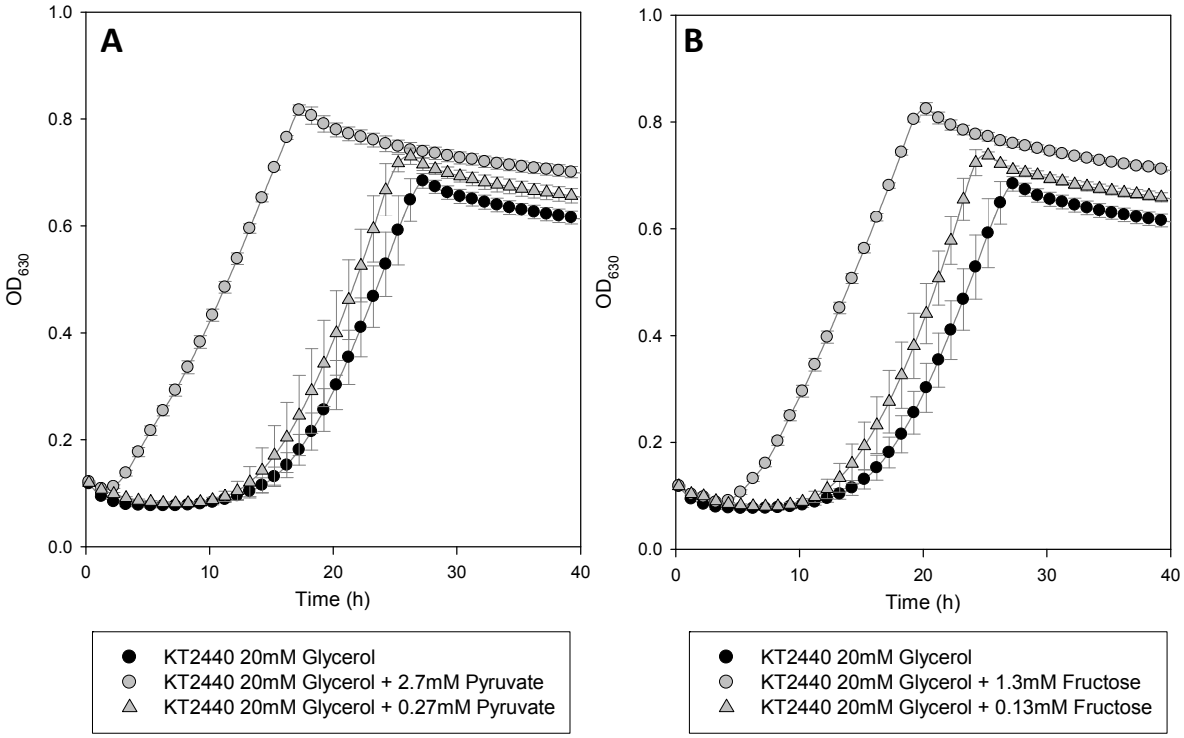
A
B
OD630
Time (h)
0.0
0.2
0.4
0.6
0.8
1.0
0
10
20
30
40
KT2440 20mM Glycerol
KT2440 20mM Glycerol + 2.7mM Pyruvate
KT2440 20mM Glycerol + 0.27mM Pyruvate
KT2440 20mM Glycerol
KT2440 20mM Glycerol + 1.3mM Fructose
KT2440 20mM Glycerol + 0.13mM Fructose